1 **Sources and Chemical Characterization of Organic Aerosol during the Summer in the**

2 **Eastern Mediterranean**

3

4

5 Evangelia Kostenidou[1,2], Kalliopi Florou[1,2], Christos Kaltsonoudis[1,2], Maria

6 Tsiflikiotou[1,2], Stergios Vratolis[3], Konstantinos Eleftheriadis[3], and Spyros N. Pandis[1,2,4]

7

8

9 [1]Institute of Chemical Engineering Sciences, ICE-HT, Patras, Greece

10 [2]Department of Chemical Engineering, University of Patras, Patras, Greece

11 [3] ERL Institute of Nuclear and Radiological Science & Technology, Energy & Safety,

12 NCRS Demokritos, Attiki, Greece

13 [4]Department of Chemical Engineering, Carnegie Mellon University, Pittsburgh, USA

14

15

16

17 **Abstract**

18 The concentration and chemical composition of non-refractory fine particulate

19 matter (NR-PM$_1$) and black carbon (BC) levels were measured during the summer of

20 2012 in the suburbs of two Greek cities, Patras and Athens, in an effort to better

21 understand the chemical processing of particles in the high photochemical activity

22 environment of the Eastern Mediterranean. The composition of PM$_1$ was surprisingly

23 similar in both areas demonstrating the importance of regional sources for the

24 corresponding pollution levels. The PM$_1$ average mass concentration was 9-14 μg m^{-3}.

25 The contribution of sulphate was around 38%, while organic aerosol (OA) contributed

26 approximately 45% in both cases. PM$_1$ nitrate levels were low (2%). The oxygen to

27 carbon (O:C) atomic ratio was 0.50±0.08 in Patras and 0.47±0.11 in Athens. In both cases

28 PM$_1$ was acidic.

29 Positive matrix factorization (PMF) was applied to the high resolution organic

30 aerosol mass spectra obtained by an Aerodyne High Resolution Time-of-Flight Aerosol

31 Mass Spectrometer (HR-ToF-AMS). For Patras five OA sources could be identified: 19%

very oxygenated OA (V-OOA), 38% moderately oxygenated OA (M-OOA), 21% biogenic oxygenated OA (b-OOA), 7% hydrocarbon-like OA (HOA-1) associated with traffic sources and 15% hydrocarbon-like OA (HOA-2) related to other primary emissions (including cooking OA). For Athens the corresponding source contributions were: V-OOA (35%), M-OOA (30%), HOA-1 (18%) and HOA-2 (17%). In both cities the major component was OOA, suggesting that under high photochemical conditions most of the OA in the Eastern Mediterranean is quite aged. The contribution of the primary sources (HOA-1 and HOA-2) was important (22% in Patras and 35% in Athens) but not dominant.

1. Introduction

Atmospheric aerosols can affect human health by causing cardiovascular and respiratory problems (Davidson et al., 2005; Pope and Dockery, 2006), they reduce visibility (Watson, 2002) and influence the energy balance of our planet (IPCC, 2013) by scattering or absorbing radiation and changing cloud reflectivity and lifetime. Submicrometer atmospheric particles mainly consist of sulphates, ammonium, organic matter, nitrates, elemental carbon and metals. Organic aerosol (OA) represents a major fraction of the submicron aerosol mass (Kanakidou et al., 2005; Zhang et al., 2007). The recent development of the Aerodyne HR-ToF-AMS (DeCarlo et al., 2006) allows high time resolution size-resolved measurements of the fine non-refractory inorganic and organic aerosol components. In addition, several techniques have been developed for the deconvolution of the AMS organic mass spectra (Zhang et al., 2011) including custom principal component analysis (Zhang et al., 2005), multiple component analysis (Zhang et al., 2007), and positive matrix factorization (PMF) (Paatero and Tapper 1994; Lanz et al., 2007). The most recent algorithm, the multilinear engine, (ME-2) (Lanz et al., 2008, Canonaco et al., 2013) is a hybrid of chemical mass balance (CMB) and bilinear models (e.g., PMF). The combination of AMS measurements with other instrumentation and the use of the corresponding source apportionment techniques can provide valuable information about the ambient aerosol sources and their chemical characterization. In this study the technique of PMF analysis on HR-ToF-AMS mass spectra is used.

62   Zhang et al. (2005) showed that summertime OA in a major urban area of the US

63   (Pittsburgh) consisted of oxygenated OA (OOA) and hydrocarbon-like OA (HOA). Lanz

64   et al. (2007) further deconvolved OOA into a more oxygenated OA (OOA-1) and a less

65   oxygenated (OOA-2) component during a summer period in Zurich. They also reported

66   for the fist time a wood burning and a charbroiling factor. Marine OA (MOA) was

67   identified by Crippa et al. (2013a) in Paris during summertime, while Schmale et al.

68   (2013) suggested the existence of an amino-acids/amine OA factor (AA-OA), a

69   methanesulfonic acid OA factor (MSA-OA), a marine oxygenated OA factor (M-OOA)

70   and a sea spray OA factor (SS-OA) on Bird Island in the South Atlantic. The major OA

71   components found usually are OOA and HOA (Ng et al., 2010). In our work the OA

72   sources are investigated, in order to characterize two urban environments in the Eastern

73   Mediterranean.

74   Most of the studies on air quality in the Eastern Mediterranean and Greece have

75   been based on filter measurements (Manoli et al., 2002; Grivas et al., 2004;

76   Papaefthymiou et al., 2005; Karanasiou et al., 2007; Chrysikou and Samara, 2009) or

77   monitoring PM mass concentrations (Chaloulakou et al., 2003; Vardoulakis and

78   Kassomenos, 2008; Yannopoulos, 2008) in major Greek cities (Athens, Thessaloniki,

79   Patras). During the past years a few field campaigns using continuous PM composition

80   measurement techniques have been conducted in rural/remote areas and urban centres in

81   Greece. At the remote site of Finokalia (Crete) factor analysis on filter samples revealed

82   three sources of coarse particles (crustal, photochemical, and marine aerosols) and two

83   additional factors in the fine mode (residual oil and secondary/combustion aerosols)

84   (Koulouri et al., 2008). For the same site no HOA was detected by PMF analysis of

85   Quadropole AMS data either in the summer or in the winter (Hildebrandt et al., 2010;

86   2011). For the city of Patras Pikridas et al. (2013) found that the transported pollution

87   accounted for 50% of the $PM_{2.5}$ during the winter and more than 70% during the rest of

88   the year. However, the Eastern Mediterranean urban environment remains not well

89   characterized.

90   In the Western Mediterranean there have been more measurement campaigns (e.g.,

91   Viana et al., 2005; Pérez et al., 2008; Pey et al., 2010; Pandolfi et al., 2014). In Barcelona

92   primary OA accounted for 59% of the OA in the late winter (Mohr et al., 2012). El

93　Haddad et al. (2013) reported that OOA contributed 80% of the OA mass in Marseille

94　during the summer, while only 5% of the OA was of industrial origin. Nicolas (2013)

95　found that OOA ranged from 70% to 85% of the total OA over a year at the Cape Corsica

96　station. For the same site the oxidation state of the OA during the summer reached

97　extremely high values with f_{44} (the fraction of the AMS m/z 44, which is an indicator of

98　the oxidation state) higher than 0.25. Thus the measurements in Western Mediterranean

99　have covered better the different types of environments compared to Eastern

100　Mediterranean.

101　　　Despite the previous efforts, there are still several knowledge gaps related to the

102　characterization of OA sources in the Mediterranean Basin. For example the contribution

103　of the primary sources is still uncertain. Fresh OA from diesel exhaust initially resembles

104　HOA but after aging may resemble semi-volatile OOA (SV-OOA) (Jimenez et al., 2009;

105　Chirico et al., 2010). Aged gas phase emissions from diesel engines, scooters and

106　biomass burning may also produce secondary OA (SOA) with mass spectra similar to

107　SV-OOA (Heringa et al., 2012). In addition, volatile organic compounds (VOCs) in

108　chamber experiments form SOA with mass spectra close to SV-OOA (Ng et al., 2010).

109　The conversion of SV-OOA to more oxidized OA is still quite difficult to reproduce in

110　the laboratory. Only recently Platt et al. (2013) showed that after 12 hours of aging of

111　gasoline Euro 5 car emissions, SOA with an O:C ratio of 0.7 was produced resembling

112　LV-OOA. In the field, Hildebrandt et al. (2010) demonstrated that primary emissions are

113　becoming highly oxygenated within 1-2 days of transport under intense photochemical

114　conditions. Recently Bougiatioti et al. (2014) showed that a large fraction of biomass

115　burning OA (BBOA) is transformed to OOA even in the dark in less than 12 hours during

116　the summer in Eastern Mediterranean. The objectives of this work are to:

117　1) characterize the chemical composition of the PM_1 in two Greek cities in the Eastern

118　Mediterranean using high time resolution instrumentation

119　2) determine the corresponding OA sources and evaluate the relative significance of the

120　primary versus the oxygenated factors

121　3) provide insights about the chemical processing of the primary PM

122　4) compare the mass spectra profiles to the corresponding profiles extracted in previous

123　studies and to

124   5) assess the overall PM$_1$ pollution in the Eastern Mediterranean in comparison with other

125   European cities.

126

127   **2 Experimental**

128   **2.1 Measurement campaign**

129   The measurements presented here were part of a larger study, which involved

130   measurements in several areas in Greece (Patras, Athens, Thessaloniki, and Finokalia)

131   both in summer and winter. In this work we will focus on the summer HR-ToF-AMS

132   measurements in Patras and Athens. More information about the summer study is

133   provided in Tsiflikiotou et al. (in preparation).

134

135   **2.2 Sampling Sites in Patras**

136   Patras has approximately 300,000 inhabitants and is located at the Gulf of Patras,

137   at the foothills of a 2 km high mountain. The major anthropogenic activities include a

138   small industrial zone about 16 km southwest of the city center and a harbor around 2.5

139   km southwest of the city. The nearest major city is Athens, around 220 km to the east.

140   Measurements in Patras were performed simultaneously at two locations: in the center of

141   the city (38° 14' 46" N, 21° 44' 08" E) and at the Institute of Chemical Engineering

142   Sciences, ICE-HT (38° 17' 52" N, 21° 48' 31" E), which is 8 km (north-east) away from

143   the city center and 1 km (south) from the Patras-Athens highway (Figure S1). The site is

144   surrounded by olive tree fields. A few small settlements are located in a distance of 1 km

145   (southwest and north-east). Most of the instrumentation was deployed at the ICE-HT

146   Institute due to space limitations in the city center station. This paper focuses only on the

147   ICE-HT measurements.

148

149   **2.3 Instrumentation in Patras**

150   A HR-ToF-AMS from Aerodyne Research Inc. (DeCarlo et al., 2006) was

151   measuring the size-resolved chemical composition of the NR-PM$_1$ aerosol species. The

152   tungsten filament for electron ionization was run at an accelerating voltage of 70 eV,

153   while the vaporizer temperature was set at 600°C. Alternative runs between V-mode

154 (single stage reflectron) and W-mode (double stage reflectron) were performed with 3

155 min of measuring time for each mode. In this paper the V-mode data are presented.

156 A Proton Transfer Reaction Mass Spectrometer (PTR-MS, Ionicon Analytik) was

157 used for the characterization of the volatile organic compounds (VOCs). More details

158 about the VOC measurements are presented in Kaltsonoudis et al. (in preparation). A

159 Scanning Mobility Particle Sizer, (SMPS, classifier model 3080, DMA model 3081, CPC

160 model 3787, TSI) was operated at a sheath flow rate of 5 L min^{-1} and a sample flow rate

161 of 1 L min^{-1}. The SMPS measured the number size distribution in the 10 - 500 nm range.

162 A Multiple-Angle Absorption Photometer (MAAP, Thermo Scientific Inc.) (Petzold and

163 Schönlinner, 2004) was used for the BC measurement. NO_x, SO_2, O_3 and CO

164 concentrations were measured by the corresponding monitors (Teledyne, models T201,

165 100E, 400E and 300E respectively).

166 A filter sampler (MetOne SAASS) was used to collect $PM_{2.5}$ samples for

167 inorganic and organic chemical composition analysis. The sampling resolution was 24 h

168 and the flow rate of each filter was 6.7 L min^{-1}. Teflon filters (Whatman 7582 004, 0.2

169 μm pore size) were used for the measurement of the inorganic anion and cation mass

170 concentrations, using two ion chromatography systems (Metrohm 761 Compact IC). Pre-

171 baked Quartz filters were used for the EC/OC measurement using a laboratory EC/OC

172 analyzer (Sunset Laboratory Inc). More details about the filter extraction procedure are

173 given by Pikridas et al. (2013) and Tsiflikiotou et al. (in preparation).

174 The HR-ToF-AMS and the PTR-MS measurements covered the period from 8 to

175 27 of June 2012, while the rest of the instrumentation provided measurements from June

176 8 to July 26, 2012. All the above mentioned instruments were located at the ICE-HT

177 campus.

178

179 **2.4 Sampling Site in Athens**

180 Athens is the most densely populated city in Greece with around 4 million

181 inhabitants. The sampling site was at Demokritos National Center for Scientific Research,

182 NCRS (37° 59' 43" N, 23° 48' 57" E), at the municipality of Agia Paraskevi. This is a

183 suburban background site 10 km from the city center located at the foothills of Ymittos

184 mountain and is surrounded by pine trees. This site is close (0.5 km) to the ring highway

185   of Ymittos and approximately 1.5 km away from the Mesogion highway to the north-

186   west. The closest residences are 0.5 km away. The relative position between Patras and

187   Athens sampling site is illustrated in Figure S2.

188

189   **2.5 Instrumentation in the Athens site**

190   For the measurements in Athens we used our mobile laboratory as a fixed station,

191   in which the HR-ToF-AMS, PTR-MS and SMPS (same models as described in session

192   2.3) were placed. An aethalometer (Magee Scientific, AE31) provided the BC

193   concentrations at 880 nm. An SMPS (classifier model 3080 TSI, custom DMA, CPC

194   model 3022, TSI) was operated at a sheath flow rate of 3 L min^{-1} and a sample flow rate

195   of 0.3 L min^{-1} and measured the number size distribution in the 10 - 660 nm range. $PM_{2.5}$

196   was collected on Teflon filters every 24 h for the inorganic composition characterization,

197   while a semi-continuous OC/EC analyzer (Field Instrument, Model 4F, Sunset

198   Laboratory Inc) equipped with a $PM_{2.5}$ inlet and an activated carbon denuder was used for

199   the $PM_{2.5}$ EC/OC measurements with a 3 hr resolution.

200   The sampling period was from 8 to 26 of July 2012. Due to technical problems

201   the HR-ToF-AMS started measuring on the July 12, 2012.

202

203   **2.6 Data Analysis**

204   For HR-ToF-AMS data analysis SQUIRREL v1.51C and PIKA v1.10C (Sueper,

205   2014) with Igor Pro 6.22A (Wavemetrics) were used. For the HR-ToF-AMS organic

206   mass spectra, we used the fragmentation table of Aiken et al. (2009).

207   PMF and ME-2 analysis (Paatero and Tapper, 1994; Lanz et al., 2007; Lanz et al.,

208   2008; Ulbrich et al., 2009; Canonaco et al., 2013) were performed using the HR-ToF-

209   AMS organic mass spectra in order to investigate the different organic aerosol sources.

210   High resolution PMF was performed using as inputs the *m/z's* 12-200 and following the

211   procedure of Ulbrich et al. (2009).

212   The Patras HR-ToF-AMS data were corrected for the collection efficiency CE

213   using the algorithm of Kostenidou et al. (2007) with a 2-hour resolution throughout the

214   campaign. A shape factor (χ) of 1 was found to be the most appropriate for this data set

215   (Supplement section 2.A, Figures S3-S4). The average CE was 0.91±0.10 and it was

216   significant higher compared to other studies, which often use a CE of 0.5. One reason

217   could be that the particles entering the HR-ToF-AMS were not dried. Drying the particles

218   usually decreases the CE because the particles bounce on the vaporizer (Matthew et al.,

219   2008). The R^2 between the 2-hour resolution CE and the 2-hour average ambient relative

220   humidity (RH) was very low (0.02). This low correlation and the high CE values can be

221   explained by the fact that the particles were acidic most of the time (see section 3.1) and

222   probably contained water during all the campaign. Comparing the PM_1 HR-ToF-AMS

223   sulphate (after CE corrections) to the $PM_{2.5}$ filter sulphate measurements a slope of 1.05

224   and a high correlation (R^2=0.98) were found as shown in Figure S5. This could indicate

225   that most of the $PM_{2.5}$ sulfate was in the submicrometer particles. The $PM_{2.5}$ sodium

226   concentration was below the detection limit, so there was practically no sodium sulphate

227   present. The average OA density estimated from the above algorithm was 1.34±0.21 g

228   cm^{-3}, which is very close to the organic density calculated for Finokalia during the

229   summer of 2008 (1.35±0.22 g cm^{-3}, Lee et al., 2010).

230   For Athens the aerosol was not dried before it entered the HR-ToF-AMS, but the

231   particles entering the SMPS were dried to maintain compatibility with long term

232   measurements performed at the site. Thus we modified the algorithm of Kostenidou et al.

233   (2007) converting the ambient HR-ToF-AMS mass distributions to dry mass distributions

234   using the relative humidity (RH) inside the sampling line and calculating the inorganic

235   aerosol water content using the Extended Aerosol Inorganic Model II (E-AIM, Carslaw et

236   al., 1995; Clegg et al., 1998; Massucci et al., 1999). As inputs to the E-AIM model we

237   used the inorganic concentrations of sulphate, ammonium and nitrate and the temperature

238   and RH at the entrance of the HR-ToF-AMS line. The algorithm was run for shape

239   factors 1-1.4 and the optimum solution was selected (i.e. the minimum of the minimum

240   error scores) which corresponded to the optimum CE, organic density, and shape factor

241   (Supplement section 2.B, Figures S6-S7). The average CE was 0.63±0.13. After applying

242   CE corrections the PM_1 HR-ToF-AMS sulphate correlated well with the $PM_{2.5}$ filter

243   sulphate (Figure S8) (R^2=0.91, slope=0.98), once more suggesting that the sulphate in the

244   1-2.5 μm range was a small fraction of the $PM_{2.5}$ sulfate. The average organic density was

245   1.15±0.36 g cm^{-3}, lower than in Patras, and the average shape factor was 1.16±0.1

246   suggesting that a lot of the particles were not spherical.

247   The angle theta (θ) between the mass spectra vectors was used as a measure of

248   their similarity (Kostenidou et al., 2009). The mass spectra are treated as vectors and the

249   angle θ is calculated by using their internal product. The lower the angle θ is the higher

250   the similarity between the two spectra.

251

252   **3 Results and Discussion**

253   **3.1 Patras**

254   The time series of the mass concentration of the NR-PM$_1$ components measured

255   by the HR-ToF-AMS and the BC in Patras are shown in Figure 1a. The average PM$_1$

256   mass concentration (not including dust) was 8.6 µg m^{-3}. On average, the organic mass

257   concentration was 3.8 µg m^{-3}, sulphate 3.3 µg m^{-3}, ammonium 0.9 µg m^{-3} and BC 0.5 µg

258   m^{-3}. Nitrate was very low around 0.1 µg m^{-3}.

259   The average OM:OC ratio was 1.80±0.10. The average diurnal profile of O:C is

260   depicted in Figure 2. O:C increased in the early morning hours (2:00-7:00 LT) and during

261   the afternoon (15:00-17:00). The OA average diurnal profile exhibited 3 peaks (Figure

262   S9a), 2 of them (around 8:00-10:00 and 21:00-23:00) were associated with primary

263   sources as the BC increased the same time as well. The OA increase at 11:00-16:00 is

264   related to the formation of secondary species as the solar intensity peaks the same time.

265   The fragments of m/z 44 and 57 represented 0.14 and 0.01 of the organic signal

266   correspondingly (Figure S10a).

267   The PM$_{2.5}$ organic carbon (OC) concentrations measured with filters was

268   converted to organic mass (OM) using the corresponding OM:OC ratio for each filter

269   sampling period provided by the HR-ToF-AMS and the two concentrations were

270   compared. Figure S11a shows the correlation between the HR-ToF-AMS and the filters

271   for organics which resulted in an R^2=0.57. This probably implies that the majority of the

272   PM$_{2.5}$ organics were in the PM$_1$ range.

273   The PM$_1$ aerosol as measured by the HR-ToF-AMS was always acidic with an

274   average inorganic cations/anions equivalent ratio of 0.75±0.07. This indicates that there

275   was no available ammonia to fully neutralize the sulphate and thus the formation of PM$_1$

276   ammonium nitrate (from ammonia and nitric acid) in the PM$_1$ was not

277   thermodynamically favorable.

278   In order to estimate the organic nitrate mass (ONit) contribution to the total nitrate

279   mass (TotNit) we followed the procedure of Farmer et al. (2010):

280
$$\frac{\text{ONit}}{\text{TotNit}} = \frac{\left(1 + R_{\text{ONit}}\right) \times \left(R_{[NO_2^+/NO^+]\text{meas}} - R_{[NO_2^+/NO^+]\text{cal}}\right)}{\left(1 + R_{[NO_2^+/NO^+]\text{meas}}\right) \times \left(R_{\text{ONit}} - R_{[NO_2^+/NO^+]\text{cal}}\right)} \quad (1)$$

281   where $R_{[NO_2^+/NO^+]\text{meas}}$ is the measured ratio of NO_2^+/NO^+ ions as a function of time,

282    $R_{[NO_2^+/NO^+]\text{cal}}$ is the ratio of NO_2^+/NO^+ ions obtained during NH_4NO_3 calibrations (0.58 on

283   average) and R_{ONit} is a fixed value set to 0.05, as the minimum ratio of NO_2^+/NO^+

284   observed in this campaign was 0.05. The average organic nitrate fraction was 0.91±0.05,

285   which suggests that most of the nitrate was in the form of organic nitrate (Figure S12a).

286   The correlation between OA and nitrate was moderate (R^2=0.38).

287

288   **3.2 Athens (Demokritos Station)**

289   On average the PM_1 mass concentration in Athens (not including dust) was 14.2 μg m^{-3}.

290   This is a different period than the one in Patras so direct comparisons could result in

291   erroneous conclusions. A detailed description and intercomparison of the various

292   measurements (including filter samples) performed in Athens and Patras is given in the

293   companion paper by Tsiflikiotou et al. (in preparation). Briefly, these authors found that

294   for the July period the mean concentrations of $PM_{2.5}$ sulphate in Patras and Athens were

295   similar, while $PM_{2.5}$ organics were higher in Patras than in Athens. Figure 1b shows the

296   time series of the concentration of the NR-PM_1 components measured by the HR-ToF-

297   AMS in Athens and the BC measured by the aethalometer. The average organic

298   concentration was 6.6 μg m^{-3}, sulphate 5.3 μg m^{-3}, ammonium 1.4 μg m^{-3} and BC 0.7 μg

299   m^{-3}. Similarly to Patras nitrate levels were low, 0.2 μg m^{-3} on average.

300   The average O:C mass ratio was 0.47±0.11, lower than in Patras (0.50), because

301   of the higher contribution of primary emissions (Section 3.3.1 and 3.3.2). The average

302   OM:OC ratio was 1.76±0.14. The diurnal cycle of O:C is shown in Figure 2 and is similar

303   to the one in Patras. The O:C exhibited two peaks one in the early morning around 3:00-

304   5:00 LT and a second in the late afternoon 17:00-20:00 LT. The OA profile is

305   characterized by three peaks (Figure S9b). Two of them, around 7:00-12:00 and 20:00-

306 24:00 are related to fresh emissions since the BC follows the same trend. A smaller

307 increase around 14:00-17:00 is probably due to photochemistry. On average f_{44} and f_{57}

308 were 0.13 and 0.02 respectively (Figure S10b).

309 The OM based on the $PM_{2.5}$ semi-continuous OC/EC measurements was

310 calculated using the OM:OC ratio provided by the HR-ToF-AMS. Figure S11b illustrates

311 the correlation for the organics between the HR-ToF-AMS and the semi-continuous

312 OC/EC samples. The measurements are in reasonable agreement (R^2=0.48), with the HR-

313 ToF-AMS providing slightly higher concentrations. The scatter observed when

314 comparing the corresponding measurements is due to a number of factors including the

315 positive and negative artifacts of filter measurements, the uncertainties of the

316 corresponding measurements and the different size ranges. The negative artifacts of the

317 filter measurements due to evaporation of the collected OA can explain the occurrence of

318 some measurements in which the $PM_{2.5}$ filter-based OA is less than the PM_1 HR-ToF-

319 AMS OA.

320 The equivalent ratio of PM_1 cations to anions (measured by the HR-ToF-AMS)

321 was on average 0.70±0.09 and thus the aerosol was acidic. Again free ammonia was not

322 enough to neutralize the sulphate and thus there was no ammonium nitrate observed in

323 the PM_1 fraction.

324 Applying equation (1) to the Athens data set (with an average $R_{[NO_2^+/NO^+]cal}$=0.68,

325 and R_{ONit} = 0.12), the organic nitrate fraction was 0.89±0.08, indicating that most of the

326 nitrate was actually organic nitrate (Figure S12b). The coefficient of determination

327 between OA and nitrate was R^2=0.62.

328

329 **3.3 OA sources**

330 **3.3.1 Patras**

331 For the PMF analysis both PMF Evaluation Tool, PET, (Lanz et al., 2008; Ulbrich

332 et al., 2009) and ME-2 (Lanz et al., 2008; Canonaco et al., 2013) solutions were

333 examined and evaluated using the HR organic mass spectra. A five factor solution was

334 chosen as the best to describe the major sources of OA in Patras. More information about

335 the choice of the solution is provided in the supplementary information (section 7.A,

336 Figures S13-S21). The factors corresponded to very oxygenated OA (V-OOA, 19%),

moderately oxygenated OA (M-OOA, 38%), biogenic oxygenated OA (b-OOA, 21%), HOA-1 (7%) and HOA-2 (15%). The V-OOA factor corresponds to the Low Volatility OOA (LV-OOA) and the M-OOA to Semivolatile OOA (SV-OOA) factors reported in previous work. The lack of a direct determination of the volatility of these factors makes the assignment of names based on their oxygen content preferable. The assignment of the factors to specific sources was based on their mass spectra and diurnal profile characteristics: V-OOA had a high contribution of m/z 44, M-OOA had a moderate m/z 44 contribution. b-OOA was characterized by both biogenic and oxidized OA signatures, HOA-1 was similar to the literature HOA factor related to traffic emissions and HOA-2 included primary cooking and aged traffic emissions. Overall, the oxygenated OA was the dominant component (78%) and the primary OA accounted for only 22%. The HR mass spectrum of each factor is illustrated in Figure 3a, while their time series are shown in Figure 4a and their average diurnal profiles in Figure 5a.

V-OOA was characterized by a high m/z 44 (~22%) with an O:C= 0.81 and is related to aged aerosol (Figure 3a). The V-OOA factor correlated well with sulphate (R^2=0.48) and ammonium (R^2=0.51), which is typical for highly oxygenated OA. Its correlation with nitrate was low (R^2=0.09). The V-OOA diurnal profile was almost flat (Figure 5a). R^2 between V-OOA and individual VOCs measured by the PTR-MS were all less than 0.13.

M-OOA had a pronounced but of lower intensity m/z 44 (~16%) and an O:C=0.54 implying aged but less oxidized particles (Figure 3a). Nitrate has been suggested as a tracer for the less oxygenated species (e.g. Lanz et al., 2007; Mohr et al., 2012), however there was very little nitrate during our measurements and most of it was organic nitrate resulting in a weak correlation between the M-OOA and nitrate (R^2=0.04). M-OOA had a very similar pattern with the solar radiation peaking at around 14:00 (local time). M-OOA had low correlation with methyl vinyl ketone (MVK) and methacrolein (MACR) (m/z 71, R^2=0.31), hydroxyacetone (m/z 75, R^2=0.29), C_5 carbonyls/2-methyl-butene-2-ol (MBO)/methacrylic acid (m/z 87, R^2=0.29), terpene oxidation products (m/z 113, R^2=0.30) and nopinone (m/z 139, R^2=0.28), (Table 1 and Figure S22). Comparing the M-OOA spectrum to the α-pinene SOA spectrum of Heringa et al. (2012) the angle theta was quite high (θ=35°), while the similarity between the M-OOA and the toluene photo-

368   oxidation SOA spectrum (Kostenidou et al., not published data) was greater (θ=16°).

369   Thus this factor may include contributions by both anthropogenic and biogenic sources.

370   The biogenic OOA factor had an f_{44}=0.13 and O:C=0.48 (Figure 3a) which

371   indicates a relatively moderate degree of oxygenation. It was characterized by a distinct

372   m/z 82 (mainly composed of $C_5H_6O^+$), an elevated m/z 53 (mostly $C_4H_5^+$) and a

373   significant contribution at m/z 39 (5%, mainly CH_3O^+). These characteristics were similar

374   to those found at a rural area in Ontario, Canada (Slowik et al., 2011), downtown Atlanta,

375   Georgia, USA (Budisulistiorini et al., 2013), in tropical rainforests in the central Amazon

376   Basin (Chen et al., 2014) and in Borneo, Malaysia (Robinson et al., 2011) and in

377   Centreville in rural Alabama (Xu et al., 2014) which were associated to secondary OA

378   produced by isoprene photooxidation. Using the HYSPLIT back trajectory model

379   (Draxler and Rolph, 2013), the mass concentration of b-OOA was almost zero when the

380   air masses were coming from the west (e.g. Ionian Sea, 11-15 June, Figure S23), while

381   M-OOA and V-OOA were still high. However, the b-OOA increased in periods (e.g. 10-

382   11 June, 16-17 and 24-26 June) when the air masses passed over the forested mountains

383   of Central Greece (Figure S23), which is an area characterized by high terpene and

384   isoprene emissions (Karl et al., 2009). This supports the biogenic character of this factor.

385   The highest concentration of b-OOA was at 6:00 in the morning on June 16th (5.4 μg m^{-3}).

386   b-OOA exhibited low correlation with isoprene (m/z 69, R^2=0.13), isoprene peroxides

387   (m/z 101, R^2=0.28) and the first generation isoprene products such as MVK and MACR

388   (m/z 71, R^2=0.21) (Table 1). However, it correlated better with acetone (m/z 59, R^2=0.35),

389   hydroxyl-acetone (m/z 75, R^2=0.41), PAN (m/z 77, R^2=0.37), nopinope (m/z 139,

390   R^2=0.39) and pinonaldehyde (m/z 151, R^2=0.30), Figure S24, which are products of

391   terpenes ozonolysis (Matsunaga et al., 2003; Holzinger et al., 2005; Lee et al., 2006).

392   HOA-1 was characterized mainly by the m/z's 39, 41, 43, 55, 57, 67, 69 and 81

393   (Figure 3a) which are typical hydrocarbon fragments of fresh traffic emissions (Zhang et

394   al., 2005; Aiken et al., 2009). Its O:C was 0.1 which is in the range found in literature

395   (the HOA factor of Mohr et al. (2012) had an O:C=0.03, while the HOA factor of Ulbrich

396   et al. (2009) had an O:C=0.18). HOA-1 had a medium correlation with BC (R^2=0.38)

397   and nitrate (R^2=0.27). The HOA-1 diurnal profile was characterized by two peaks during

398   the morning (8:00) and evening rush hours (21:00) (Figure 5a). HOA-1 correlated

399   moderately with benzene (m/z 79, R^2=0.36), toluene (m/z 93, R^2=0.35), xylenes (m/z 107,

400   R^2=0.37), C_9 aromatic compounds (m/z 121, R^2=0.45). The correlation with NO_x was

401   relatively low (R^2=0.26).

402   The HOA-2 O:C was 0.21. The HOA-2 spectrums was characterized among

403   others by the $m/z's$ 39, 41, 43, 44, 55, 57 and 67 (Figure 3a) which are features of

404   cooking organic aerosol, COA (Ge et al., 2011a, b; Crippa et al., 2013a, b). However, the

405   reported COA spectra (e.g. Ge et al., 2011a, b; Crippa et al., 2013a, b) have lower

406   contributions at m/z 44 (0.011-0.022), indicating less oxygenation. The f_{44} in the HOA-2

407   mass spectrum was 0.034 which implies that this factor may also contain species that

408   have been oxidized to some degree. The HOA-2 diurnal profile had a small peak around

409   14:00 and a higher one around 22:00, which are consistent with the Greek lunch and

410   dinner periods (Figure 5a). Thus, the HOA-2 in Patras is mainly due to charbroiling of

411   meat cooking OA. The correlation between HOA-2 and BC, nitrate, benzene, toluene,

412   xylenes and C_9 aromatic compounds was moderate (R^2=0.38, 0.38, 0.33, 0.30, 0.33 and

413   0.43 correspondingly).

414   During June 16-23 the wind speed was relatively high (average 5.3 m s^{-1})

415   compared to the rest of the sampling days (average 2.5 m s^{-1}). The contribution of the

416   local sources (HOA-1 and HOA-2) was less than 9% of the OA during that windy period

417   compared to 28% during the remaining days (Figure 4a).

418

419   **3.3.2 Athens**

420   Four OA factors could be identified in the Athens HR-ToF-AMS data set: V-

421   OOA (35%), M-OOA (30%), HOA-1 (18%) and HOA-2 (17%). A detailed description of

422   the reasons for this selection can be found in the supplement (section 7.B, Figures S25-

423   S33). The corresponding mass spectra are provided in Figure 3b. The time series of the

424   four PMF factors are shown in Figure 4b, while their diurnal cycles in Figure 5b.

425   Similarly to Patras the contribution of the oxygenated OA in Athens was high (65%),

426   while the primary sources contributed 35%.

427   The very oxidized OA (V-OOA) had an f_{44}=0.18 and O:C=0.68 and showed a

428   good correlation with sulphate (R^2=0.53) and ammonium (R^2=0.50) consistent with the

429   aged character of this factor. The diurnal profile of the V-OOA (Figure 5b) was

430 characterized by a peak around 15:00-18:00, which is probably associated with

431 production of this component in the afternoon over the region. At the same time M-OOA

432 decreased, which indicates that V-OOA is a product of photochemical processing. V-

433 OOA correlated with formic acid (m/z 47, R^2=0.47), hexenal (m/z 99, R^2=0.42), isoprene

434 peroxides (m/z 101, R^2=0.35), terpene oxidation products (m/z 113, R^2=0.40), and

435 heptanal (m/z 115, R^2=0.42) (Table 1 and Figure S34).

436   The moderately oxidized OA (M-OOA) was characterized by an f_{44}=0.14 and

437 O:C=0.56 and exhibited a weak correlation with sulphate, ammonium and nitrate

438 (R^2=0.17, 0.17 and 0.13 respectively). M-OOA increased during the day with a maximum

439 at 12:00-14:00, following the diurnal profile of solar radiation, which implies relatively

440 fast photochemical reactions. M-OOA had a second peak during the night around

441 midnight, which could be an indication of nighttime production or condensation due to

442 the change in temperature between day and night (the average temperature at noon was

443 32°C, while during the night it decreased to around 21°C). M-OOA did not show any

444 correlation (R^2 less than 0.07) with the measured VOCs.

445 The HOA-1 O:C was 0.07. Surprisingly it had a rather weak correlation with BC

446 (R^2=0.05) and it also showed a low correlation with nitrate (R^2=0.13). The HOA-1 diurnal

447 profile had 2 peaks, a small increase during the morning (7:00) and a larger peak in the

448 evening hours (20:00), consistent with the contribution of traffic emissions. HOA-1 did

449 not correlate with VOCs characteristic of traffic such as benzene, toluene and xylenes

450 (the R^2 values were correspondingly 0.15, 0.13 and 0.16) and inorganic gases as NO_x

451 (R^2= 0.06). The HOA-1 mass spectrum and time series were very stable for 2 to 5

452 factorial solutions and for f_{peaks} values from -1 to 1. The R^2 between the HOA-1 of the

453 selected solution and the HOA-1 of the solutions of 2, 3 and 5 factors was always greater

454 than 0.973 (both for the time series and the mass spectra). This weak correlation between

455 the HOA-1 factor and other primary organic pollutants indicates that their concentrations

456 were not dominated by the same sources. For example HOA-1 possibly originated mostly

457 from passenger cars and scooters. In Greece the car-to-scooter ratio is around 3 to 1 and

458 using the Platt et al. (2014) primary OA emissions from two-stroke engines the scooter

459 emissions are expected to be a significant OA source. BC mainly originated from diesel

460 vehicles. Another potential BC source could be shipping emissions from Piraeus (15 km

461   south-west of the sampling site) and Rafina (17 km east) ports. However, during high BC

462   concentration periods (around 10:00 LT) the wind was from the north (Figure S35). Thus,

463   the main source of BC was probably diesel vehicles.

464   The location of the sampling site and the inhomogeneity of the surrounding areas,

465   in combination with the wind direction changes have confounded these effects. The rose

466   plots of HOA-1, BC, NO_x and benzene for wind speeds greater than 1 m s^{-1} indicated that

467   BC, NO_x and benzene had the same origin, while HOA-1 did not. For example at 8:00

468   LT the HOA-1 was on average coming from southwest (Figure S35-S38) likely from the

469   ring highway of Ymittos, while BC, NO_x and benzene from the north probably influenced

470   by the Mesogion highway.

471   HOA-2 had an O:C=0.24 and exhibited a good correlation with BC (R^2=0.57).

472   HOA-2 also correlated well with nitrate (R^2=0.75) implying that organic nitrate

473   compounds were possibly emitted or produced along with this OA type. The HOA-2

474   profile had 2 peaks at around 11:00 and 22:00. The second peak is characteristic of Greek

475   dinner period, thus part of HOA-2 could be attributed to meat cooking OA. However, the

476   first peak can not be explained by the Greek lunch period. Although it could contain

477   cooking emissions from canteens or caterings which start cooking earlier than the typical

478   Greek lunchtime, it still does not explain the good correlation with BC. Greek cooking

479   emissions have a low BC/OA ratio (unpublished measurements). Thus HOA-2 may

480   include sources other than cooking. The correlation with the BC implies that HOA-2 and

481   BC had the same origin. Comparing the HOA-2 mass spectrum with aged POA or SOA

482   emissions from other sources such as α-pinene, wood burning, scooter and diesel

483   (Heringa et al., 2012) the angles θ were 19, 19, 28, 17° respectively. This indicates that

484   HOA-2 could include aged diesel emissions since α-pinene is not associated with BC and

485   there were no observed biomass burning events during the sampling period. The HOA-2

486   factor correlated with the *m/z* 43 (R^2=0.43), acetone (*m/z* 59, R^2=0.44), methyl ethyl

487   ketone (MEK, *m/z* 73, R^2=0.49), benzene (*m/z* 79, R^2=0.62), toluene (*m/z* 93, R^2=0.54),

488   xylenes (*m/z* 107, R^2=0.56), C_9 aromatic compounds (*m/z* 121, R^2=0.58) and C_{10} aromatic

489   compounds (*m/z* 135, R^2=0.55). It also had a good correlation with NO_x (R^2=0.58).

490   Trying rotations in the *f$_{peak}$* range -1 to 1 the correlations between the factors

491   HOA-1 and HOA-2 and traffic markers such as BC and toluene practically did not

492   change. In addition using a fixed HOA spectrum (the HOA mass spectrum of Aiken et al.

493   (2009) and the HOA mass spectrum found in Athens during winter, unpublished results)

494   with a=0.1 the correlation between HOA-1 and BC did not improve. All these suggest

495   that our conclusions are robust to the details of the PMF process. Our explanation is that

496   the correlations are affected also by the locations of the various sources around the

497   receptor site and the corresponding wind directions. The fact that these area sources

498   (gasoline cars, diesel cars, cooking activities) did not have a homogeneous spatial

499   distribution can lead to these rather unexpected results.

500

501   **3.3.3 Comparison of the PMF factors in the two cities**

502   The mass spectra of the V-OOA factors in the two cities were almost the same

503   (θ=6.7^{o}). However, Athens V-OOA exhibited lower f_{44} and O:C ratio (0.18 and 0.68

504   correspondingly) compared to Patras V-OOA (0.22 and 0.81 respectively). This

505   difference could be partially due to the different periods of the two measurements.

506   The two M-OOA mass spectra were even more similar to each other (θ=5.4^{o}). A

507   high correlation was also observed between the two HOA-2 mass spectra (θ=5.9^{o}). The

508   Athens HOA-2 was slightly more oxygenated (O:C=0.24), as the oxygenated part of m/z

509   43 was more elevated, 65%, compared to 51% observed in Patras HOA-2 and the f_{44} was

510   just slightly higher (0.07), while in Patras HOA-2 was 0.06.

511   The two HOA-1 factors exhibited a lower correlation with each other (θ=22.8^{o}).

512   The main differences were at m/z 41, 43, 55, 57, 69, 71, 81, 83 and 85 which were more

513   abundant in the Athens HOA-1 spectrum, while in the Patras spectrum the f_{44} was higher

514   (0.04) compared to Athens (0.02). In Patras HOA-1 spectrum m/z 57 was lower in

515   comparison with m/z 55. The O:C in Athens HOA-1 was a little lower (0.07) than in

516   Patras HOA-1 (0.10).

517

518   **3.3.4 Comparing the PMF factors with other studies**

519   Table 2 shows comparisons of the mass spectra of the factors found in the two

520   cities with selected PMF factors from the literature (Aiken et al., 2009; Docherty et al.,

521   2011; Sun et al., 2011; Robinson et al., 2011; Heringa et al., 2012; Mohr et al., 2012, Ge

522 et al., 2012a, b; Crippa et al., 2013a, b; Budisulistiorini et al., 2013; Xu et al., 2014) that

523 have all been extracted using the fragmentation table of Aiken et al. (2009).

524   The two V-OOA factors were quite similar with LV-OOA at Riverside (Docherty

525 et al., 2011), θ=8-10°, and with LV-OOA at New York City (Sun et al., 2011), θ=11-14°.

526 They also showed good correlation with LV-OOA measured in Barcelona (Mohr et al.,

527 2012) and Paris (Crippa et al., 2013a, b) θ=13-19°.

528   M-OOA had moderate to low agreement with the majority of the literature

529 profiles. The lowest angle θ (around 22-24°) corresponded to the comparison with the

530 SV-OOA found in Mexico City (Aiken et al., 2009). It did however resemble (θ=13-16°)

531 the toluene SOA spectrum (Kostenidou et al., not published data).

532   The b-OOA factor in Patras correlated moderately with α-pinene SOA, θ=29°,

533 (Heringa et al., 2012) and the isoprene factor found in Alabama, θ=28°, (Xu et al.,

534 submitted). However, it had low correlation with the Factor 82, θ=47°, found in Malaysia

535 (Robinson et al., 2011) and the IEPOX OA factor extracted in Atlanta, θ=76°,

536 (Budisulistiorini et al., 2013).

537   The HOA-1 factors correlated well with most of the literature HOA profiles,

538 θ=10-25°.The highest angles (24 and 25°) corresponded to the comparison with Paris

539 during the winter (Crippa et al., 2013b). The major differences were in the *m/z's* 44 and

540 28 which were higher than in Paris, *m/z's* 29 and 43 which were lower compared to Paris

541 and *m/z* 39 which was absent in Paris probably due to the unit mass resolution spectra

542 used as input for the Crippa et al. (2013) PMF analysis.

543   The HOA-2 mass spectra resembled the COA factor extracted in New York City,

544 θ=11-14°, (Sun et al., 2011) and the SOA from diesel VOCs emissions, θ=17°, (Heringa

545 et al., 2012).

546   Figure S39 summarizes Patras and Athens OA measurements and PMF factors in

547 the Ng triangle (Ng et al., 2010). All the data fall within the triangle.

548

549 **3.4 Discussion**

550   In both cities the composition of NR-PM$_1$ was surprisingly similar. Organic

551 contributions in Patras and Athens were around 45%, which is similar to other areas in

552 Europe: London (UK) 46%, mountain Taunus (Germany) 59%, Melpitz (Germany) 59%,

553 Mace Head (Ireland) 39%, Po Valley (Italy) 33%, and Paris (France) 50% (Cubison et al.,

554 2006; Hings et al., 2007; Poulain et al., 2011; Dall'Osto et al., 2010; Saarikoski et al.,

555 2012; Crippa et al., 2013a). With 38%, sulphate made a larger contribution compared to

556 other studies in Europe during the summer: London 31%, mountain Taunus 24%, Mace

557 Head 32%, Melpitz 22%, Po Valley 9%, and Paris 25% (Cubison et al., 2006; Hings et al.,

558 2007; Dall'Osto et al., 2010; Poulain et al., 2011; Saarikoski et al., 2012; Crippa et al.,

559 2013a). Nitrate contributed very little (less than 2%) and was mostly attributed to

560 organonitrate compounds, in contrast with other European studies where nitrate ranged

561 from 6% (Melpitz) to 39% (Po Valley) (Poulain et al., 2011; Saarikoski et al., 2012) and

562 mainly was ammonium nitrate. The absence of particulate nitrate in PM_1 was also

563 observed at Finokalia (Hildebrandt et al., 2010) and is characteristic of the Eastern

564 Mediterranean. Ammonia levels in this region are quite low (Wichink Kruit et al., 2012)

565 to fully neutralize the existing relatively high sulphate.

566 The O:C ratios (0.50 for Patras and 0.47 for Athens) were moderately high. The

567 O:C ratio at Finokalia was 0.8 (Hildebrandt et al., 2010), at Cape Corsica 0.9 (Nicolas,

568 2013), while in Paris 0.38 (Crippa et al., 2013a).

569 In both cities the OOA was the dominant OA component (78% in Patras and 65%

570 in Athens). This fraction is within the range that has been measured in previous summer

571 studies in the Mediterranean. For example, the OOA at Finokalia was 100% of the OA

572 (Hildebrandt et al., 2010), in Marseille accounted for 80% (El Haddad et al., 2013), at

573 Cape Corsica 80-85% (Nicolas, 2013), while in Po Valley 61% (Saarikoski et al., 2012).

574 In Athens 35% of the OA was V-OOA, while in Patras only 19% of the OA was

575 attributed to V-OOA. In addition the V-OOA in Athens was increasing in the afternoon,

576 suggesting its production either locally or regionally. In Patras V-OOA had an almost flat

577 diurnal profile. This difference could be attributed to the different air masses that arrive to

578 each site. According to back trajectory analysis, based on FLEXPART (Stohl et al., 2005)

579 (Figure S40) and HYSPLIT (Draxler and Rolph 2013) during most of the sampling days

580 in Athens the air masses had spent considerable time over the source-poor Aegean Sea,

581 while the majority of the air masses that arrived in Patras were continental and passed

582 over the mountains of Central Greece.

583   Given the location of the two sites, one would expect to find a marine OA (MOA)

584   factor. The S:C ratio estimated by the AMS is often underestimated in the presence of

585   organosulfates (Farmer et al., 2010; Docherty et al., 2011). To avoid such artifacts we

586   investigated the contribution of MOA applying a constrained solution in the ME-2 using

587   the MOA mass spectrum of Crippa et al. (2013) with a=0.1. For Patras the average MOA

588   concentration for 4, 5, and 6 factors was around 0.04 μg m^{-3} corresponding to 1 percent of

589   the OA mass. For Athens the MOA concentration for the 3, 4 and 5 factor solutions was

590   approximately 0.25 μg m^{-3} (3.7 percent of the OA mass). So if MOA was indeed present

591   its contribution to OA was quite low.

592

4 Conclusions

594   During the summer of 2012 the air pollution in Patras (June) and Athens (July)

595   was monitored continuously. The sum of the NR-PM$_1$ and BC concentration was on

596   average 8.6 μg m^{-3} in Patras and 14.2 μg m^{-3} in Athens. However, the aerosol composition

597   was quite similar in both areas: 45% OA, 38% sulphate, 11% ammonium, 1% nitrate

598   (mostly organic) and 5% BC indicating the importance of regional sources. In both cities

599   the fine aerosol was acidic, which is consistent with the low ammonia levels in the

600   Eastern Mediterranean.

601   For Patras the average O:C ratio was 0.50±0.08, while in Athens 0.47±0.11. In

602   both cities oxygenated OA was the major component of organic aerosol (78% in Patras

603   and 65% in Athens), indicating the impact of regional pollution in Mediterranean. OOA

604   included a moderately oxygenated OA and a very oxygenated OA component. In Patras a

605   biogenic oxidized OA factor could be identified, which was related to air masses passing

606   over the forests of Central Greece. A primary OA factor (HOA-2) was found in both

607   cities attributed to primary emissions such as meat cooking. This factor may also contain

608   oxygenated primary emissions (e.g., aged diesel emissions). Hydrocarbon-like OA

609   mainly from traffic emissions was also indentified, accounting only for 7-18% of the OA

610   and indicating that new emission control technologies applied to vehicles during the last

611   decade have reduced dramatically the levels of the corresponding primary OA.

612

621

References

623   Aiken, A. C., Salcedo, D., Cubison, M. J., Huffman, J. A., DeCarlo, P. F., Ulbrich, I. M.,

624   Docherty, K. S., Sueper, D., Kimmel, J. R., Worsnop, D. R., Trimborn, A., Northway, M.,

625   Stone, E. A.,   Schauer, J. J.,   Volkamer, R. M.,   Fortner, E.,   de Foy, B.,   Wang, J.,

626   Laskin, A., Shutthanandan, V., Zheng, J., Zhang, R., Gaffney, J., Marley, N. A., Paredes-

627   Miranda, G.,   Arnott, W. P.,   Molina, L. T.,   Sosa, G.,   and   Jimenez, J. L.: Mexico City

628   aerosol analysis during MILAGRO using high resolution aerosol mass spectrometry at

629   the urban supersite (T0) – Part 1: Fine particle composition and organic source

630   apportionment, Atmos. Chem. Phys., 9, 6633-6653, 2009.

631

632   Bougiatioti, A., Stavroulas, I., Kostenidou, E., Zarmpas, P., Theodosi, C., Kouvarakis, G.,

633   Canonaco, F.,   Prévôt, A. S. H.,   Nenes, A.,   Pandis, S. N.,   and   Mihalopoulos, N.:

634   Processing of biomass-burning aerosol in the eastern Mediterranean during summertime,

635   Atmos. Chem. Phys., 14, 4793-4807, 2014.

636

637   Budisulistiorini, S. H., Canagaratna, M. R., Croteau, P. L., Marth, W. J., Baumann, K.,

638   Edgerton, E. S., Shaw, S. L., Knipping, E. M., Worsnop, D. R., Jayne, J. T., Gold, A., and

639   Surratt, J. D.: Real-time continuous characterization of secondary organic aerosol derived

640   from isoprene epoxydiols in downtown Atlanta, Georgia, using the Aerodyne Aerosol

641   Chemical Speciation Monitor, Environ. Sci. Technol., 47, 5686–5694, doi:

642   10.1021/es400023n, 2013.

643

644 Canonaco, F., Crippa, M., Slowik, J. G., Baltensperger, U., and Prévôt, A. S. H.: SoFi, an
645 IGOR-based interface for the efficient use of the generalized multilinear engine (ME-2)
646 for the source apportionment: ME-2 application to aerosol mass spectrometer data,
647 Atmos. Meas. Tech., 6, 3649-3661, 2013.

648

649 Carslaw, K. S., Clegg, S. L., and Brimblecombe, P.: A thermodynamic model of the
650 system $HCl-HNO_3-H_2SO_4-H_2O$, including solubilities of HBr, from <200K to 328 K, J.
651 Phys. Chem., 99, 11557–11574, 1995.

652

653 Chaloulakou A., Kassomenos, P., Spyrellis, N., Demokritou, P., and Koutrakis, P.:
654 Measurements of PM_{10} and $PM_{2.5}$ particle concentrations in Athens, Greece, Atmos.
655 Environ., 37, 649–660, 2003.

656

657 Chen, Q., Farmer, D. K., Rizzo, L. V., Pauliquevis, T., Kuwata, M., Karl, T. G.,
658 Guenther, A., Allan, J. D., Coe, H., Andreae, M. O., Pöschl, U., Jimenez, J. L., Artaxo, P.,
659 and Martin, S. T.: Fine-mode organic mass concentrations and sources in the Amazonian
660 wet season (AMAZE-08), Atmos. Chem. Phys. Discuss., 14, 16151-16186, 2014.

661

662 Chirico, R., DeCarlo, P. F., Heringa, M. F., Tritscher, T., Richter, R., Prévôt, A. S. H.,
663 Dommen, J., Weingartner, E., Wehrle, G., Gysel, M., Laborde, M., and Baltensperger,
664 U.: Impact of aftertreatment devices on primary emissions and secondary organic aerosol
665 formation potential from in-use diesel vehicles: results from smog chamber experiments,
666 Atmos. Chem. Phys., 10, 11545–11563, 2010.

667

668 Chrysikou L.P. and Samara C.: Seasonal variation of the size distribution of urban
669 particulate matter and associated organic pollutants in the ambient air, Atmos. Environ.,
670 43, 4557- 4569, 2009.

671

672 Clegg, S., Brimblecombe, L., P. and Wexler, A. S.: A thermodynamic model of the
673 system $H^+-NH_4^+-SO_4^{2-}-NO_3^--H_2O$ at tropospheric temperatures. J. Phys. Chem. A102,
674 2137–2154, doi: 10.1021/jp973043j, 1998.

675

676 Crippa M., El Haddad I., Slowik J., G., DeCarlo P. F., Mohr, C., Heringa, M., F, Chirico,
677 R., Marchand, N., Sciare, J., Urs, B., and Prévôt, A. S. H.: Identification of marine and
678 continental aerosol sources in Paris using high resolution aerosol mass spectrometry, J.
679 Geophys. Res, doi: 118, 1950-1963, doi: 10.1002/jgrd.50151, 2013a.

680

681 Crippa, M., DeCarlo, P. F., Slowik, J. G., Mohr, C., Heringa, M. F., Chirico, R., Poulain,
682 L., Freutel, F., Sciare, J., Cozic, J., Di Marco, C. F., Elsasser, M., Jose, N., Marchand,
683 N., Abidi, E., Wiedensohler, A., Drewnick, F., Schneider, J., Borrmann, S., Nemitz, E.,
684 Zimmermann, R., Jaffrezo, J.-L., Prévôt, A. S. H., and Baltensperger, U.: Wintertime
685 aerosol chemical composition and source apportionment of the organic fraction in the
686 metropolitan area of Paris, Atmos. Chem. Phys., 13, 961–981, 2013b.

687

688 Cubison, M. J., Alfarra, M. R., Allan, J., Bower, K. N., Coe, H., McFiggans, G. B.,
689 Whitehead, J. D., Williams, P. I., Zhang, Q., Jimenez, J. L., Hopkins, J., and Lee, J.: The
690 characterization of pollution aerosol in a changing photochemical environment, Atmos.
691 Chem. Phys., 6, 5573-5588, 2006.

692

693 Dall'Osto, M., Ceburnis, D., Martucci, G., Bialek, J., Dupuy, R., Jennings, S. G.,
694 Berresheim, H., Wenger, J., Healy, R., Facchini, M. C., Rinaldi, M., Giulianelli, L.,
695 Finessi, E., Worsnop, D., Ehn, M., Mikkilä, J., Kulmala, M., and O'Dowd, C. D.: Aerosol
696 properties associated with air masses arriving into the North East Atlantic during the
697 2008 Mace Head EUCAARI intensive observing period: an overview, Atmos. Chem.
698 Phys., 10, 8413-8435, 2010.

699

700 Davidson, C. I., Phalen, R. F., and Solomon, P. A.: Airborne particulate matter and
701 human health: A review, Aerosol Sci. Tech., 39, 737–749, 2005.

702

703 DeCarlo, P.F., Kimmel, J. R., Trimborn, A., Northway, M. J., Jayne, J. T., Aiken, A. C.,
704 Gonin, M., Fuhrer, K., Horvath, T., Docherty, K., Worsnop, D. R., and Jimenez, J. L.:

705 Field-Deployable, High-Resolution, Time-of-Flight Aerosol Mass Spectrometer,
706 Analytical Chemistry, 78, 8281-8289, 2006.

707

708 Docherty, K. S., Aiken, A. C., Huffman, J. A., Ulbrich, I. M., DeCarlo, P. F., Sueper, D.,
709 Worsnop, D. R., Snyder, D. C., Peltier, R. E., Weber, R. J., Grover, B. D., Eatough, D. J.,
710 Williams, B. J., Goldstein, A. H., Ziemann, P. J., and Jimenez, J. L.: The 2005 Study of
711 Organic Aerosols at Riverside (SOAR-1): Instrumental intercomparisons and fine particle
712 composition, Atmos. Chem. Phys., 11, 12387-12420, 2011.

713

714 Draxler, R. R., and Rolph, G. D., 2013. HYSPLIT (HYbrid Single-Particle Lagrangian
715 Integrated Trajectory) Model access via NOAA ARL READY Website
716 (http://ready.arl.noaa.gov/HYSPLIT.php). NOAA Air Resources Laboratory, Silver
717 Spring, MD.

718

719 El Haddad, I., D'Anna, B., Temime-Roussel, B., Nicolas, M., Boreave, A., Favez, O.,
720 Voisin, D., Sciare, J., George, C., Jaffrezo, J.-L., Wortham, H., and Marchand, N.:
721 Towards a better understanding of the origins, chemical composition and aging of
722 oxygenated organic aerosols: case study of a Mediterranean industrialized environment,
723 Marseille, Atmos. Chem. Phys., 13, 7875-7894, 2013.

724 Farmer, D.K., Matsunaga, A., Docherty, K. S., Surratt, J. D., Seinfeld, J. H., Ziemann P.
725 J., and Jimenez, J. L., Response of an aerosol mass spectrometer to organonitrates and
726 organosulfates and implications for atmospheric chemistry. Proceedings of the National
727 Academy of Sciences, 107, 6670-6675, doi: 10.1073/pnas.0912340107, 2010.

728 Ge, X., Setyan, A., Sun, Y., and Zhang, Q.: Primary and secondary organic aerosols in
729 Fresno, California during wintertime: Results from high resolution aerosol mass
730 spectrometry, J. Geophys. Res., 117, D19301, 10.1029/2012JD018026, 2012a.

731 Ge, X., Zhang, Q., Sun, Y., Ruehl, C. R., and Setyan, A.: Effect of aqueous-phase
732 processing on aerosol chemistry and size distribution in Fresno, California, during
733 wintertime, Environ. Chem., 9, 221-235, 10.1071/EN11168, 2012b.

734 Grivas, G., Chaloulakou, A, Samara, C., and Spyrellis, N.: Spatial and temporal variation
735 of PM_{10} mass concentrations within the greater area of Athens, Greece, Water, Air and
736 Soil Pollution, 158, 357-371, 2004.

737

738 Heringa, M. F., DeCarlo, P. F., Chirico, R., Tritscher, T., Clairotte, M., Mohr, C.,
739 Crippa, M., Slowik, J. G., Pfaffenberger, L., Dommen, J., Weingartner, E.,
740 Prévôt, A. S. H., and Baltensperger, U.: A new method to discriminate secondary organic
741 aerosols from different sources using high-resolution aerosol mass spectra, Atmos. Chem.
742 Phys., 12, 2189-2203, 2012.

743

744 Hildebrandt, L., Engelhart, G. J., Mohr, C., Kostenidou, E., Lanz, V. A., Bougiatioti, A.,
745 DeCarlo, P. F., Prévôt, A. S. H., Baltensperger, U., Mihalopoulos, N., Donahue, N. M.,
746 and Pandis, S. N.: Aged organic aerosol in the Eastern Mediterranean: the Finokalia
747 Aerosol Measurement Experiment – 2008, Atmos. Chem. Phys., 10, 4167–4186, 2010.
748

749 Hildebrandt, L., Kostenidou, E., Lanz, V. A., Prévôt, A. S. H., Baltensperger, U.,
750 Mihalopoulos, N., Laaksonen, A., Donahue, N. M., and Pandis, S. N.: Sources and
751 atmospheric processing of organic aerosol in the Mediterranean: insights from aerosol
752 mass spectrometer factor Analysis, Atmos. Chem. Phys., 11, 12499–12515, 2011.

753

754 Hings S.S., Walter, S., Schneider, J., Borrmann, S., and Drewnick, F.: Comparison of a
755 Quadrupole and a Time-of-Flight Aerosol Mass Spectrometer during the Feldberg
756 Aerosol Characterization Experiment 2004, Aerosol Science and Technology, 41, 679 -
757 691, 2007.

758

759 Holzinger, R., Lee, A., Paw, K. T., and Goldstein, U. A. H.: Observations of oxidation
760 products above a forest imply biogenic emissions of very reactive compounds, Atmos.
761 Chem. Phys., 5, 67-75, doi: 10.5194/acp-5-67-2005, 2005.

762

763   IPCC: Climate Change 2013 – The Physical Science Basis, Contribution of Working

764   Group I to the Fourth Assessment Report of the IPCC, Cambridge University Press,

765   Cambridge, 2013.

766

767   Jimenez, J. L., Canagaratna, M. R., Donahue, N. M., Prévôt, A. S. H., Zhang, Q., Kroll, J.

768   H., DeCarlo, P. F., Allan, J. D., Coe, H., Ng, N. L., Aiken, A. C., Docherty, K. S.,

769   Ulbrich, I. M., Grieshop, A. P., Robinson, A. L., Duplissy, J., Smith, J. D., Wilson, K. R.,

770   Lanz, V. A., Hueglin, C., Sun, Y. L., Tian, J., Laaksonen, A., Raatikainen, T., Rautiainen,

771   J., Vaattovaara, P., Ehn, M., Kulmala, M., Tomlinson, J. M., Collins, D. R., Cubison, M.

772   J., Dunlea, E. J., Huffman, J. A., Onasch, T. B., Alfarra, M. R., Williams, P. I., Bower, K.,

773   Kondo, Y., Schneider, J., Drewnick, F., Borrmann, S., Weimer, S., Demerjian, K.,

774   Salcedo, D., Cottrell, L., Griffin, R., Takami, A., Miyoshi, T., Hatakeyama, S., Shimono,

775   A., Sun, J. Y., Zhang, Y. M., Dzepina, K., Kimmel, J. R., Sueper, D., Jayne, J. T.,

776   Herndon, S. C., Trimborn, A. M., Williams, L. R., Wood, E. C., Middlebrook, A. M.,

777   Kolb, C. E., Baltensperger, U., and Worsnop, D. R.: Evolution of organic aerosols in the

778   atmosphere, Science, 326, 1525–1529, 2009.

779

780   Holzinger, R., Lee, A., Paw, K. T., and Goldstein, U. A. H.: Observations of oxidation

781   products above a forest imply biogenic emissions of very reactive compounds, Atmos.

782   Chem. Phys., 5, 67-75, 2005.

783

784   Kanakidou, M., Seinfeld, J. H., Pandis, S. N., Barnes, I., Dentener, F. J., Facchini, M. C.,

785   Van Dingenen, R., Ervens, B., Nenes, A., Nielsen, C. J., Swietlicki, E., Putaud, J. P.,

786   Balkanski, Y., Fuzzi, S., Horth, J., Moortgat, G. K., Winterhalter, R., Myhre, C. E. L.,

787   Tsigaridis, K., Vignati, E., Stephanou, E. G., and Wilson, J.: Organic aerosol and global

788   climate modeling: a review, Atmos. Chem. Phys., 5, 1053–1123, 2005.

789

790   Kaltsonoudis, C., Kostenidou, E., Florou, K., Psichoudaki, M., and Pandis, S. N.:

791   Temporal variability of VOCs in the Eastern Mediterranean (in preparation).

792

793   Karanasiou, A. A., Sitaras, I. E., Siskos, P. A., and Eleftheriadis, K.: Size distribution and
794   sources of trace metals and n-alkanes in the Athens urban aerosol during summer, Atmos.
795   Environ., 41, 2368–2381, 2007.
796

797   Karl, M., Guenther, A., Köble, R., Leip, A., and Seufert, G.: A new European plant-
798   specific emission inventory of biogenic volatile organic compounds for use in
799   atmospheric transport models, Biogeosciences, 6, 1059-1087, 2009.
800

801   Kostenidou, E., Pathak, R. K., and Pandis, S. N.: An algorithm for the calculation of
802   secondary organic aerosol density combining AMS and SMPS data, Aerosol Sci.
803   Technol., 41, 1002–1010, 2007.
804

805   Kostenidou, E., Lee, B. H., Engelhart, G. J., Pierce, J. R., and Pandis, S. N.: Mass spectra
806   deconvolution of low, medium and high volatility biogenic secondary organic aerosol,
807   Environ. Sci. Technol., 43, 4884–4889, 2009.
808

809   Koulouri, E., Saarikoski, S., Theodosi, C., Markaki, Z., Gerasopoulos, E., Kouvarakis, G.,
810   Makela, T., Hillamo, R., and Mihalopoulos, N.: Chemical composition and sources of
811   fine and coarse aerosol particles in the Eastern Mediterranean, Atmos. Environ., 42,
812   6542–6550, 2008.
813

814   Lanz, V. A., Alfarra, M. R., Baltensperger, U., Buchmann, B., Hueglin, C., and Prévôt, A.
815   S. H.: Source apportionment of submicron organic aerosols at an urban site by factor
816   analytical modeling of aerosol mass spectra, Atmos. Chem. Phys., 7, 1503–1522, 2007.

817   Lanz, V. A., Alfarra, M. R., Baltensperger, U., Buchmann, B., Hueglin, C., Szidat, S.,
818   Wehrli, M. N., Wacker, L., Weimer, S., Caseiro, A., Puxbaum, J., and Prévôt, A. S. H.:
819   Source attribution of submicron organic aerosols during wintertime inversions by
820   advanced factor analysis of aerosol mass spectra, Environ. Sci. Technol., 42, 214-220,
821   2008.

822   Lee, A., Goldstein, A. H., Keywood, M. D., Gao, S.,Varutbangkul, V., Bahreini, R., Ng,

823   N. L., Flagan, R. C., and Seinfeld, J. H.: Gas-phase products and secondary aerosol yields

824   from the ozonolysis of ten different terpenes, J. Geophys. Res., 111, D07302, doi:

825   10.1029/2005JD006437, 2006.

826   Lee, B. H., Kostenidou, E., Hildebrandt, L., Riipinen, I., Engelhart, G. J., Mohr, C.,

827   DeCarlo, P. F., Mihalopoulos, N., Prévôt, A. S. H., Baltensperger, U. and Pandis S. N.:

828   Measurement of the ambient organic aerosol volatility distribution: application during the

829   Finokalia Aerosol Measurement Experiment (FAME-2008), Atmos. Chem. Phys., 10,

830   12149–12160, 2010.

831   Manoli E., Voutsa D. and Samara C.: Chemical characterization and source

832   identification/apportionment of fine and coarse air particles in Thessaloniki, Greece,

833   Atmos. Environ., 36, 949-961, 2002.

834

835   Massucci, M., Clegg, S. L., and Brimblecombe, P.: Equilibrium partial pressures,

836   thermodynamic properties of aqueous and solid phases, and Cl_2 production from aqueous

837   HCl and HNO_3 and their mixtures, J. Phys. Chem. A 103, 4209 4226, doi:

838   10.1021/jp9847179, 1999.

839   Matsunaga, S., Mochida, M., and Kawamura, K.: Growth of organic aerosols by biogenic

840   semi-volatile carbonyls in the forest atmosphere, Atmos. Environ., 37, 2045–2050, 2003.

841   Matthew, B. M., Middlebrook, A. M., and Onasch, T. B.: Collection efficiencies in an

842   Aerodyne Aerosol Mass Spectrometer as a function of particle phase for laboratory

843   generated aerosols, Aerosol Sci. Technol., 42, 884–898, 2008.

844   Mohr, C., DeCarlo, P. F., Heringa, M. F., Chirico, R., Slowik, J. G., Richter, R., Reche,

845   C., Alastuey, A., Querol, X., Seco, R., Peñuelas, J., Jimenez, J. L., Crippa, M.,

846   Zimmermann, R., Baltensperger, U., and Prévôt, A. S. H.: Identification and

847   quantification of organic aerosol from cooking and other sources in Barcelona using

848   aerosol mass spectrometer data, Atmos. Chem. Phys., 12, 1649–1665, 2012.

849

850   Nicolas, J. : Caractérisation physico-chimique de l'aérosol troposphérique en

851   Méditerranée : Sources et Devenir, Ph.D. thesis, Université de Versailles Saint-Quentin-

852   en-Yvelines, Ecole Doctorale des Sciences de l'Environnement d'Ile-de-France, Paris,

853   France, 2013.

854

855   Ng, N.L., Canagaratna, M. R., Zhang, Q., Jimenez, J. L., Tian, J., Ulbrich, I. M., Kroll, J.

856   H., Docherty, K. S., Chhabra, P. S., Bahreini, R., Murphy, S. M., Seinfeld, J. H.,

857   Hildebrandt, L., Donahue, N. M., DeCarlo, P. F., Lanz, V. A., Prévôt, A. S. H., Dinar, E.,

858   Rudich, Y., and Worsnop D. R.: Organic aerosol components observed in northern

859   hemispheric datasets measured with Aerosol Mass Spectrometry. Atmos. Chem. Phys, 10,

860   4625-4641, 2010.

861

862   Paatero, P. and Tapper, U.: Positive matrix factorization – a nonnegative factor model

863   with optimal utilization of error-estimates of data values, Environmetrics, 5, 111–126,

864   1994.

865

866   Pandolfi, M., Querol, X., Alastuey, A., Jimenez, J. L., Jorba, O., Day, D., Ortega, A.,

867   Cubison, M. J., Comerón, A., Sicard, M., Mohr, C., Prévôt, A. S. H., Minguillón, M. C.,

868   Pey, J., Baldasano, J. M., Burkhart, J. F., Seco, R., Peñuelas, J., van Drooge, B. L.,

869   Artiñano, B., Di Marco, C., Nemitz, E., Schallhart, S., Metzger, A., Hansel, A., Llorente,

870   J., Ng, S., Jayne, J., and Szidat, S.: Effects of sources and meteorology on particulate

871   matter in the Western Mediterranean Basin: An overview of the DAURE campaign, J.

872   Geophys. Res. Atmos., 119, 4978–5010, doi: 10.1002/2013JD021079, 2014.

873

874   Papaefthymiou, H., Kritidis, P., Anousis, J., and Sarafidou, J.: Comparative assessment of

875   natural radioactivity in fallout samples from Patras and Megalopolis, Greece, J. of

876   Environomental Radioactivity, 78, 249-265, 2005.

877

878   Pérez, N., Pey, J., Castillo, S., Viana, M., Alastuey, A., and Querol, X.: Interpretation of

879   the variability of levels of regional background aerosols in the Western Mediterranean,

880   Science of the Total Environment, 407, 527-540, 2008.

881

882 Petzold, A., and Schönlinner, M: Multi-angle absorption photometry – a new method for

883 the measurement of aerosol light absorption and atmospheric black carbon, J. Aerosol

884 Sci., 35, 421-441, 2004.

885

886 Pey, J., Pérez, N., Querol, X., Alastuey, A., Cusack, M., and Reche, C.: Intense winter

887 atmospheric pollution episodes affecting the Western Mediterranean, Science of the Total

888 Environment, 408, 1951-1959, 2010.

889 Pikridas, M., Tasoglou, A., Florou, K., and Pandis, S. N.: Characterization of the origin

890 of fine particulate matter in a medium size urban area in the Mediterranean, Atmos.

891 Environ., 80, 264–274, 2013.

892

893 Platt, S. M., El Haddad, I., Zardini, A. A., Clairotte, M., Astorga, C., Wolf, R.,

894 Slowik, J. G., Temime-Roussel, B., Marchand, N., Ježek, I., Drinovec, L., Močnik, G.,

895 Möhler, O., Richter, R., Barmet, P., Bianchi, F., Baltensperger, U., and Prévôt, A. S. H.:

896 Secondary organic aerosol formation from gasoline vehicle emissions in a new mobile

897 environmental reaction chamber, Atmos. Chem. Phys., 13, 9141-9158, 2013.

898

899 Platt, S.M., El Haddad, I., Pieber, S. M., Huang, R-J., Zardini, A. A., Clairotte, M.,

900 Suarez-Bertoa, R., Barmet, P., Pfaffenberger, L., Wolf, R., Slowik, J.G., Fuller, S. J.,

901 Kalberer, M., Chirico, R., Domme, J., Astorga, C., Zimmermann, R., Marchand, N.,

902 Hellebust, S., Temime-Roussel, B., Baltensperger U., and. Prévôt A.S.H.: Two-stroke

903 scooters are a dominant source of air pollution in many cities, Nature Communications, 5,

904 doi: 10.1038/ncomms4749, 2014.

905

906 Pope, C. A. and Dockery, D. W.: Health effects of fine particulate air pollution: Lines

907 that connect, J. Air Waste Manage., 56, 709–742, 2006.

908

909   Poulain, L., Spindler, G., Birmili, W., Plass-Dülmer, C., Wiedensohler, A., and

910   Herrmann, H.: Seasonal and diurnal variations of particulate nitrate and organic matter at

911   the IfT research station Melpitz, Atmos. Chem. Phys., 11, 12579-12599, 2011.

912

913   Robinson, N. H., Hamilton, J. F., Allan, J. D., Langford, B., Oram, D. E., Chen, Q.,

914   Docherty, K., Farmer, D. K., Jimenez, J. L., Ward, M. W., Hewitt, C. N., Barley, M. H.,

915   Jenkin, M. E., Rickard, A. R., Martin, S. T., McFiggans, G., and Coe, H.: Evidence for a

916   significant proportion of secondary organic aerosol from isoprene above a maritime

917   tropical forest, Atmos. Chem. Phys., 11, 1039–1050, 2011.

918

919   Saarikoski, S., Carbone, S., Decesari, S., Giulianelli, L., Angelini, F., Canagaratna, M.,

920   Ng, N. L., Trimborn, A., Facchini, M. C., Fuzzi, S., Hillamo, R., and Worsnop, D.:

921   Chemical characterization of springtime submicrometer aerosol in Po Valley, Italy,

922   Atmos. Chem. Phys., 12, 8401-8421, 2012.

923

924   Schmale, J., Schneider, J., Nemitz, E., Tang, Y. S., Dragosits, U., Blackall, T. D., Trathan,

925   P. N., Phillips, G. J., Sutton, M., and Braban C. F.: Sub-Antarctic marine aerosol:

926   significant contributions from biogenic sources, Atmos. Chem. Phys., 13, 8669–8694,

927   2013.

928

929   Slowik, J. G., Brook, J., Chang, R. Y.-W., Evans, G. J., Hayden, K., Jeong, C.-H., Li, S.-

930   M., Liggio, J., Liu, P. S. K., McGuire, M., Mihele, C., Sjostedt, S., Vlasenko, A., and

931   Abbatt, J. P. D.: Photochemical processing of organic aerosol at nearby continental sites:

932   contrast between urban plumes and regional aerosol, Atmos. Chem. Phys., 11, 2991–3006,

933   2011.

934

935   Stohl, A., Forster, V., Frank, A., Seibert, P., & Wotawa, G.: Technical Note: The

936   Lagrangian particle dispersion model FLEXPART version 6.2, Atmos. Chem. Phys., 5,

937   2461–2474, 2005.

938

939   Sueper, D.: ToF-AMS High Resolution Analysis Software – Pika, online available at:
940   http://cires.colorado.edu/jimenez-group/ ToFAMSResources/ToFSoftware, last access: 1
941   December 2014.

942

943   Sun, Y. L., Zhang, Q., Schwab, J. J., Demerjian, K. L., Chen, W. N., Bae, M. S., Hung, H.
944   M., Hogrefe, O., Frank, B., Rattigan, O. V., and Lin, Y. C.: Characterization of the
945   sources and processes of organic and inorganic aerosols in New York city with a high-
946   resolution time-of-flight aerosol mass spectrometer, Atmos. Chem. Phys., 11, 1581–1602,
947   2011.

948

949   Tsiflikiotou, T., Papanastasiou, D., Zarmpas, P., Paraskevopoulou, D., Diapouli, E.,
950   Kostenidou, E., Kaltsonoudis, C., Bougiatioti, A., Theodosi, C., Kouvarakis, G.,
951   Liakakou, E., Vassilatou, V., Siakavaras, D., Biskos, G., Eleftheriadis, K., Gerasopoulos,
952   E., Mihalopoulos, N., and Pandis, S. N.: Spatial distribution of summertime particulate
953   matter and its composition in Greece (in preparation).

954

955   Ulbrich, I. M., Canagaratna, M. R., Zhang, Q., Worsnop, D. R., and Jimenez, J. L.:
956   Interpretation of organic components from Positive Matrix Factorization of aerosol mass
957   spectrometric data, Atmos. Chem. Phys., 9, 2891–2918, 2009.

958

959   Vardoulakis S. and Kassomenos P.: Sources and factors affecting PM10 levels in two
960   European cities: Implications for local air quality management, Atmos. Environ., 4142,
961   3949-3963, 2008.

962

963   Viana, M., Pérez, C., Querol, X., Alastuey, A., Nickovic, S., and Baldasano J. M.: Spatial
964   and temporal variability of PM levels and composition in a complex summer atmospheric
965   scenario in Barcelona (NE Spain), Atmos. Environ., 39, 5343-5361, 2005.

966

967   Watson, J. G.: Visibility: Science and regulation, J. Air Waste Manage., 52, 628–713,
968   2002.

969

970 Wichink Kruit, R. J., Schaap, M., Sauter, F. J., van Zanten, M. C., and van Paul, W. A.
971 J.: Modeling the distribution of ammonia across Europe including bi-directional surface-
972 atmosphere exchange, Biosciences, 9, 5261–5277, 2012.

973

974 Yannopoulos, P.C.: Long-term assessment of airborne particulate concentrations in Patras,
975 Greece, Fresenius Environ. Bull., 17, 608-616, 2008.

976

977 Xu, L., Guo, H., Boyd, C. M., Klein, M., Bougiatioti, A., Cerully, K, M., Hite, J. R.,
978 Isaacman-VanWertz, G., Kreisberg, N. M., Knote, C., Olson, K., Koss, A., Goldstein, A.
979 H., Hering, S. V., de Gouw, J., Baumann, K., Lee, S-H., Nenes, A., Weber, R. J., Ng, N.
980 L.: Effects of anthropogenic emissions on aerosol formation from isoprene and
981 monoterpenes in the Southeastern United States, P. Natl. Acad. Sci., 112, 37-42, doi:
982 10.1073/pnas.1417609112, 2014.

983

984 Zhang, Q., Alfarra, M. R., Wornsop, D. R., Allan, J. D., Coe, H., Canagaratna, M., and
985 Jimenez, J. L.: Deconvolution and quantification of hydrocarbon-like and oxygenated
986 organic aerosols based on aerosol mass spectrometry, Environ. Sci. Technol., 39, 4938-
987 4952, 2005.

988 Zhang, Q., Jimenez, J. L., Canagaratna, M. R., Allan, J. D., Coe, H., Ulbrich, I., Alfarra,
989 M. R., Takami, A., Middlebrook, A. M., Sun, Y. L., Dzepina, K., Dunlea, E., Docherty,
990 K., De- Carlo, P. F., Salcedo, D., Onasch, T., Jayne, J. T., Miyoshi, T., Shimono, A.,
991 Hatakeyama, S., Takegawa, N., Kondo, Y., Schneider, J., Drewnick, F., Borrmann, S.,
992 Weimer, S., Demerjian, K., Williams, P., Bower, K., Bahreini, R., Cottrell, L., Griffin, R.
993 J., Rautiainen, J., Sun, J. Y., Zhang, Y. M., and Worsnop, D. R.: Ubiquity and dominance
994 of oxygenated species in organic aerosols in anthropogenically-influenced Northern
995 Hemisphere midlatitudes, Geophys. Res. Lett., 34, L13801, doi: 10.1029/2007gl029979,
996 2007.

997

998   Zhang, Q., Jimenez, J., Canagaratna, M., Ulbrich, I., Ng, N., Worsnop, D., and Sun, Y.:

999   Understanding atmospheric organic aerosols via factor analysis of aerosol mass

1000   spectrometry: a review, Anal. Bioanal.Chem., 401, 3045-3067, 2011.

1001

1002

1003

1004

1005

1006

1007

1008

1009

1010

1011

1012

1013

1014

1015

1016

1017

1018

1019

1020

1021

1022

1023

1024

1025

1026

1027

1028 **Table 1**. Correlations[a] of the M-OOA and b-OOA factors (Patras) and the V-OOA factor

1029 (Athens) with various VOCs measured by the PTR-MS.

R^2	Patras M-OOA	Patras b-OOA	Athens V-OOA
m/z 43	0.29	0.13	0.39
m/z 47 (formic acid)	0.21	0.09	0.47
m/z 59 (acetone, glyoxal)	0.21	0.35	0.32
m/z 71 (MVK, MACR)	0.31	0.21	0.20
m/z 73 (MEK)	0.24	0.25	0.29
m/z 75 (hydroxyacetone)	0.29	0.41	0.30
m/z 77 (PAN)	0.16	0.37	0.16
m/z 81 (terpenes)	0.19	0.26	0.12
m/z 87 (MBO, C5, methacrylic acid)	0.29	0.31	0.38
m/z 95 (2 vinyl furan, phenol)	0.17	0.31	0.36
m/z 99 (hexenal)	0.19	0.30	0.42
m/z 101 (isoprene hyperoxides,hexanal)	0.17	0.28	0.35
m/z 103 (MPAN)	0.23	0.28	-
m/z 113 (chlorobenzene, terpenes +O$_3$)	0.30	0.37	0.40
m/z 115 (heptanal)	0.16	0.32	0.42
m/z 137 (monoterpenes)	0.20	0.24	0.1
m/z 139 (nopinone)	0.28	0.39	0.19
m/z 151 (pinonaldehyde)	0.17	0.30	0.17

1030 [a]All correlations are significant at the $p=0.05$ level.

1031

1032

1033

1034

1035

1036

1037

1038
1039
1040

1041   **Table 2**. Correlations between PMF factors from Patras and Athens and PMF factors

1042   from selected studies using both the angle theta and R^2 (in parenthesis).

	Angle in degrees (and R^2) **with V-OOA Patras**	**Angle in degrees** (and R^2) **with V-OOA Athens**
LV-OOA Mexico City[1]	21 (0.86)	20 (0.87)
LV-OOA Riverside[2]	10 (0.97)	8 (0.98)
LV-OOA Barcelona[3]	18 (0.90)	16 (0.92)
LV-OOA Paris (SIRTA) summer[4]	19 (0.89)	15 (0.93)
OOA Paris (SIRTA), winter[5]	13 (0.95)	15 (0.93)
LV-OOA New York City[6]	14 (0.94)	11 (0.96)
LV-OOA Fresno[7,8]	36 (0.64)	30 (0.73)

1043

	Angle in degrees (and R^2) **with M-OOA Patras**	**Angle in degrees** (and R^2) **with M-OOA Athens**
SV-OOA Mexico City[1]	24 (0.81)	22 (0.84)
SV-OOA Riverside[2]	42 (0.48)	39 (0.53)
SV-OOA Barcelona[3]	33 (0.66)	31 (0.69)
SV-OOA Paris (SIRTA) summer[4]	42 (0.48)	39 (0.53)
SV-OOA New York City[6]	30 (0.73)	27 (0.77)
α-pinene ozonolysis SOA aged[9]	35 (0.62)	32 (0.67)
Toluene photooxidation (HONO) SOA[10]	16 (0.93)	13 (0.95)

1044

	Angle in degrees (and R^2) **with HOA-1 Patras**	**Angle in degrees** (and R^2) **with HOA-1 Athens**
HOA Mexico City[1]	13 (0.94)	14 (0.93)
HOA Riverside[2]	20 (0.86)	10 (0.96)
HOA Barcelona[3]	22 (0.84)	11 (0.96)
HOA Paris (SIRTA) summer[4]	16 (0.92)	18 (0.90)
HOA Paris (SIRTA), winter[5]	25 (0.79)	24 (0.81)
HOA New York City[6]	12 (0.95)	10 (0.97)
HOA Fresno[7,8]	11 (0.96)	11 (0.96)

1045

|	**Angle in degrees** (and R^2) **with HOA-2 Patras**	**Angle in degrees** (and R^2) **with HOA-2 Athens**
COA Barcelona[3]	77 (0.01)	77 (0.01)
COA Paris (SIRTA), summer[4]	30 (0.68)	34 (0.6)
COA Paris (SIRTA), winter[5]	30 (0.74)	28 (0.70)
COA Paris (LHVP), winter[5]	27 (0.76)	31 (0.70)
COA New York City[6]	11 (0.96)	14 (0.93)
COA Fresno[7,8]	28 (0.72)	33 (0.64)
Aged VOCs diesel emissions[9]	17 (0.90)	17 (0.90)
α-pinene ozonolysis SOA aged[9]	20 (0.86)	19 (0.87)
Toluene photooxidation (HONO) SOA[10]	26 (0.79)	23 (0.84)

1046

1047
1048
1049
1050

	Angle in degrees (and R^2) with b-OOA Patras
α-pinene ozonolysis SOA aged[9]	29 (0.73)
Factor 82[11]	47 (0.40)
IEPOX OA[12]	76 (0.01)
Isoprene-OA[13]	28 (0.75)

1051
1052   [1]Aiken et al. (2009), [2]Docherty et al. (2011), [3]Mohr et al. (2012), [4]Crippa et al. (2013a), [5]Crippa et al.
1053   (2013b), [6]Sun et al. (2011), [7,8]Ge et al. (2012a,b), [9]Heringa et al. (2012), [10]Kostenidou et al., (not published
1054   data),[11]Robinson et al. (2011), [13]Budisulistiorini et al. (2013), [13]Xu et al., (2014).
1055
1056
1057
1058
1059
1060
1061
1062
1063
1064
1065
1066
1067
1068
1069
1070
1071
1072
1073
1074
1075
1076
1077
1078
1079
1080
1081
1082
1083
1084
1085
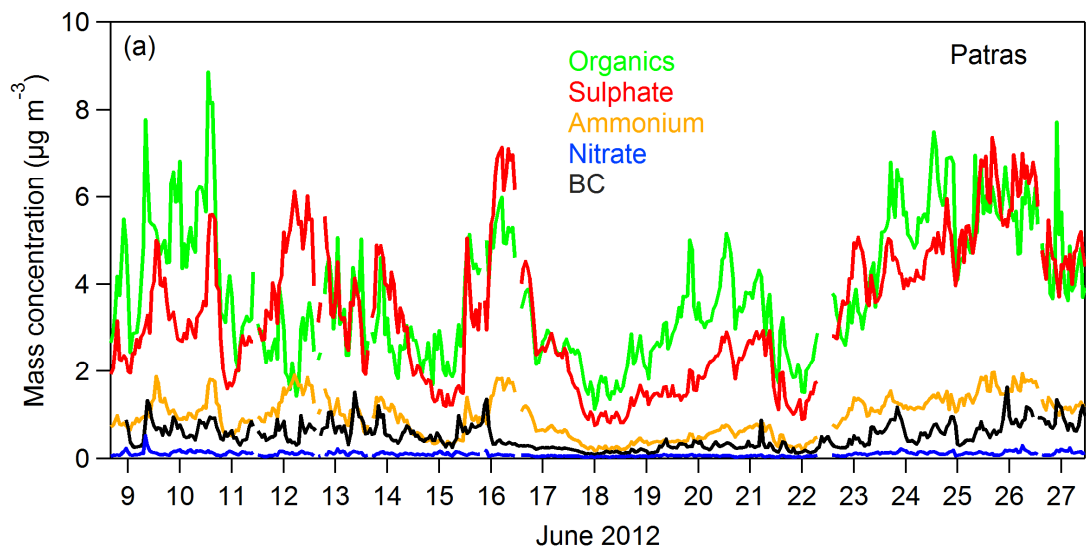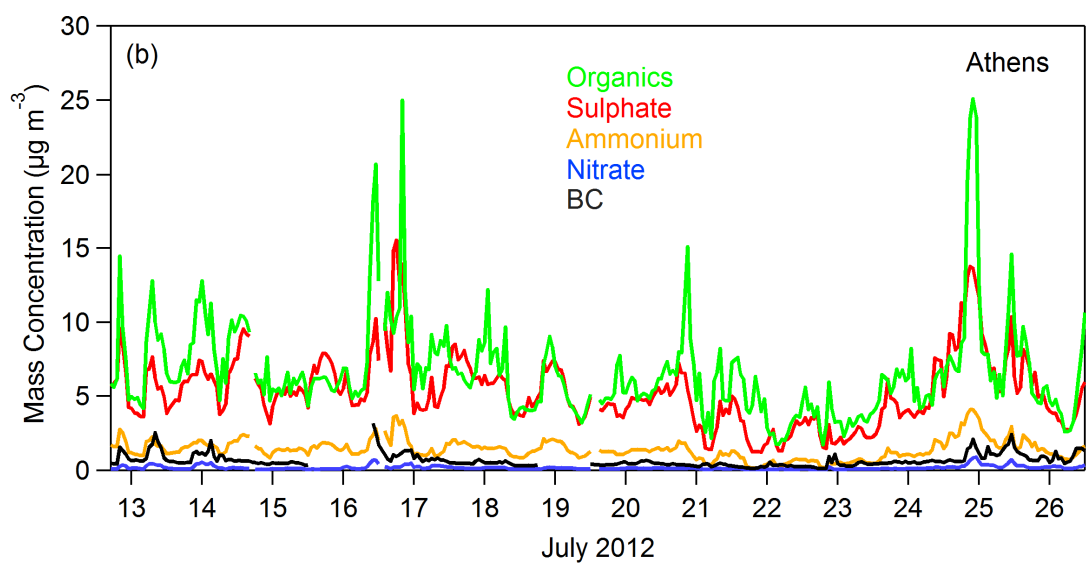
Figure 1. Time series of organics, sulphate, ammonium and nitrate mass concentration measured by the HR-ToF-AMS (corrected for the CE) and BC a) for Patras and b) for Athens. The BC was provided by MAAP for Patras measurements and by an aethalometer for Athens.
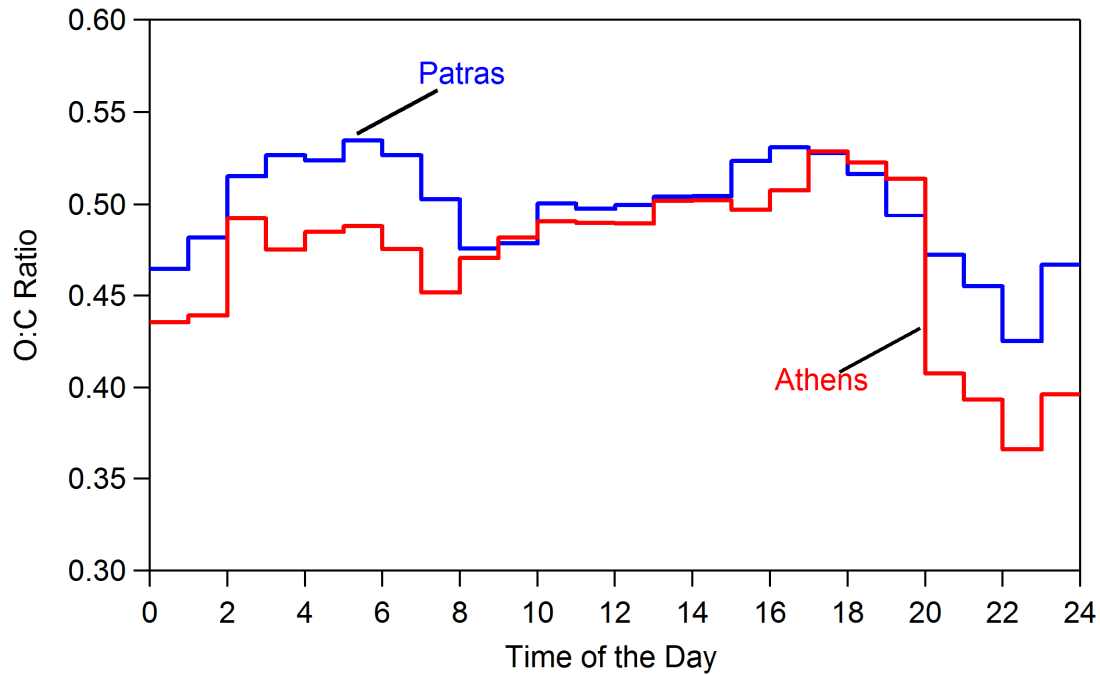
1101
1102
1103
1104 **Figure 2**. Diurnal profile of O:C ratio for Patras (blue line) and Athens (red line) data set.

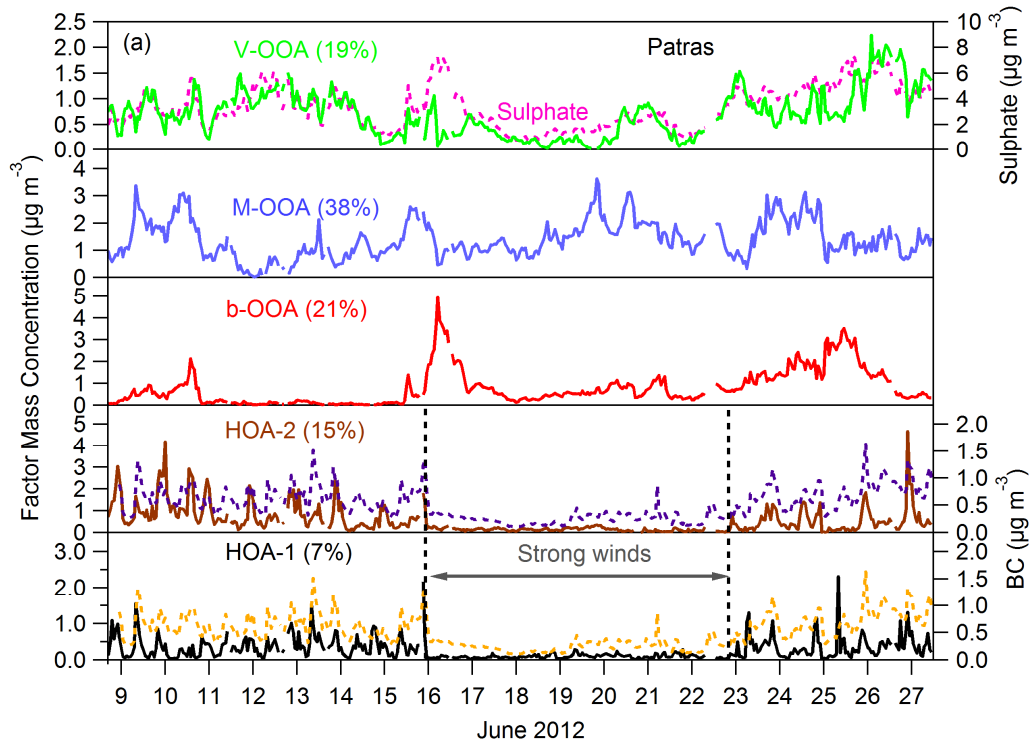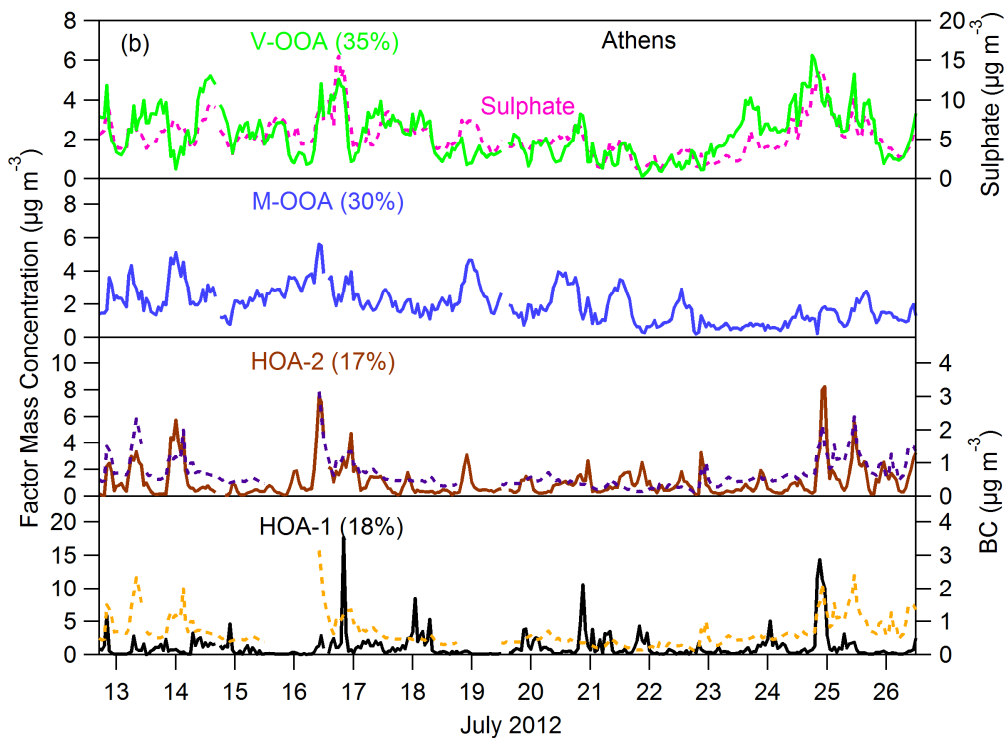1105 The O:C was calculated with the Aiken et al. (2009) fragmentation table.

1106
1107
1108
1109
1110
1111
1112
1113
1114
1115
1116
1117
1118
1119
1120
1121
1122
1123
1124
1125
1126
1127
1128
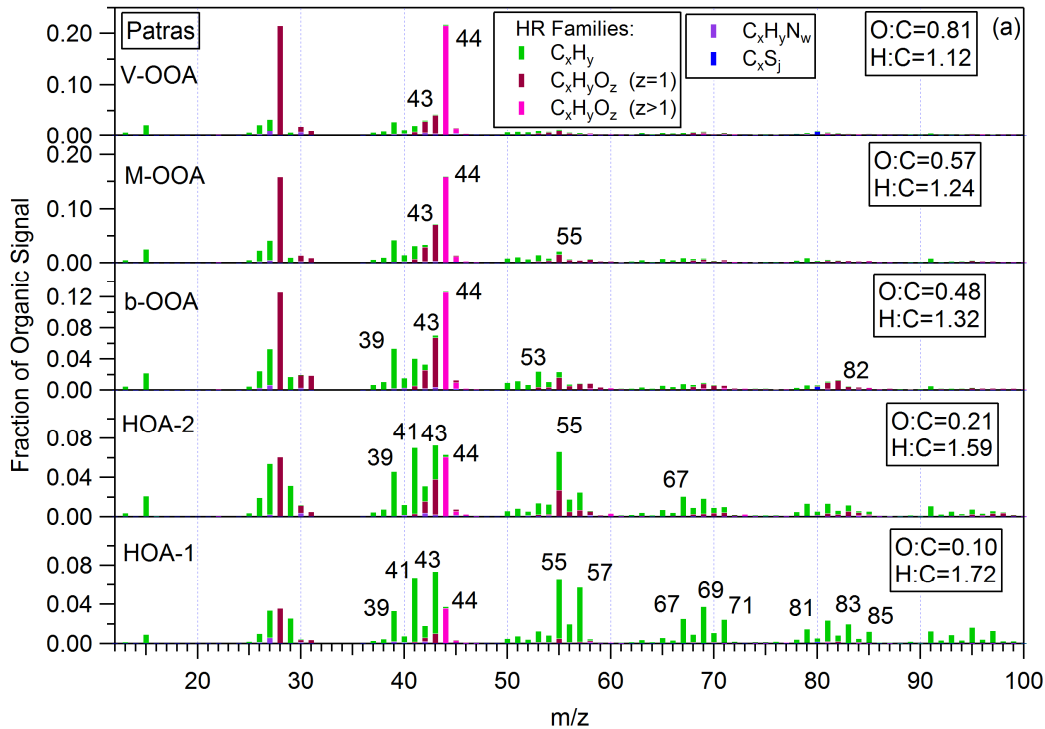
1129
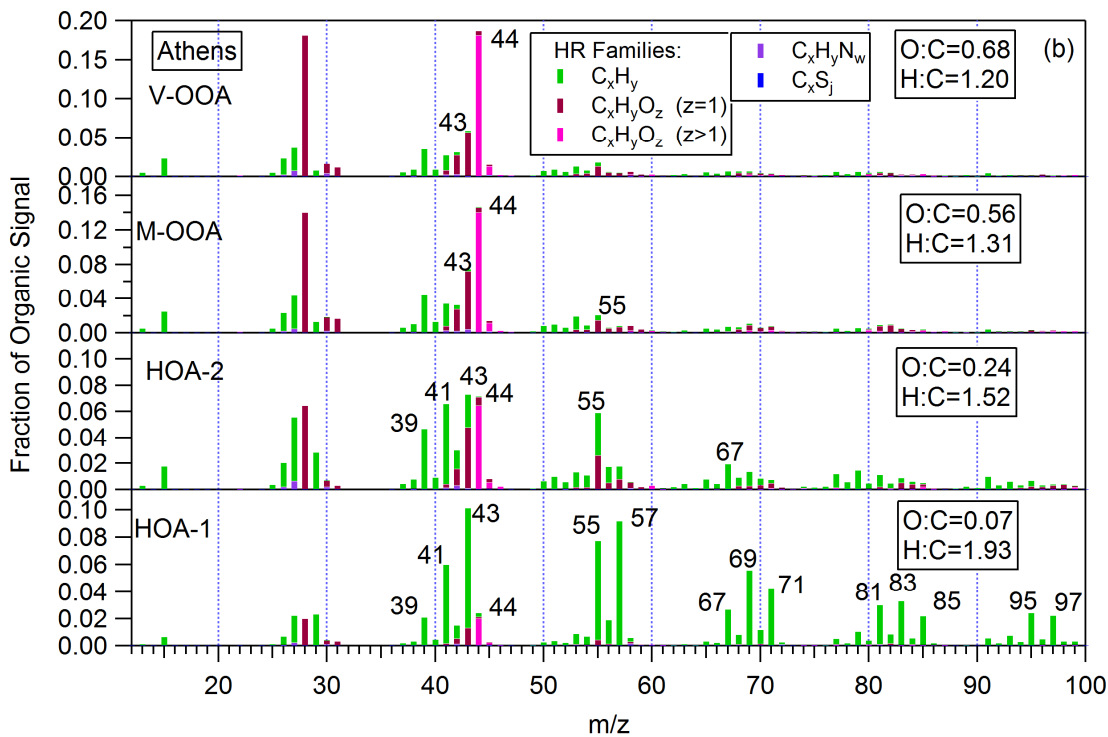
1130
1131
1132 **Figure 3**. HR mass spectra profiles of the sources found a) in Patras and b) in Athens.
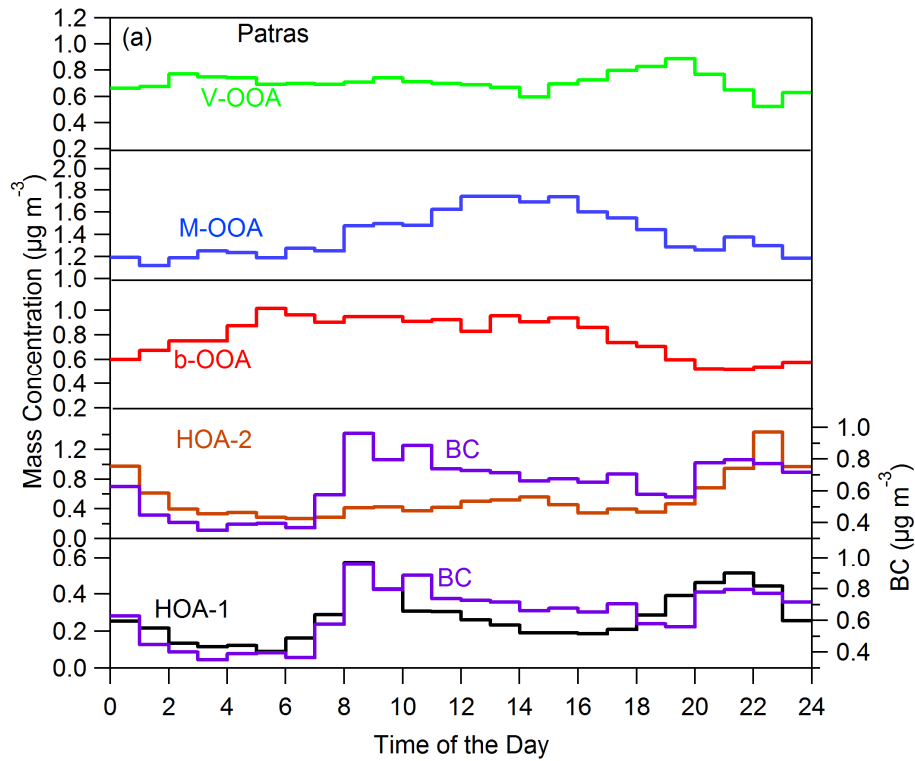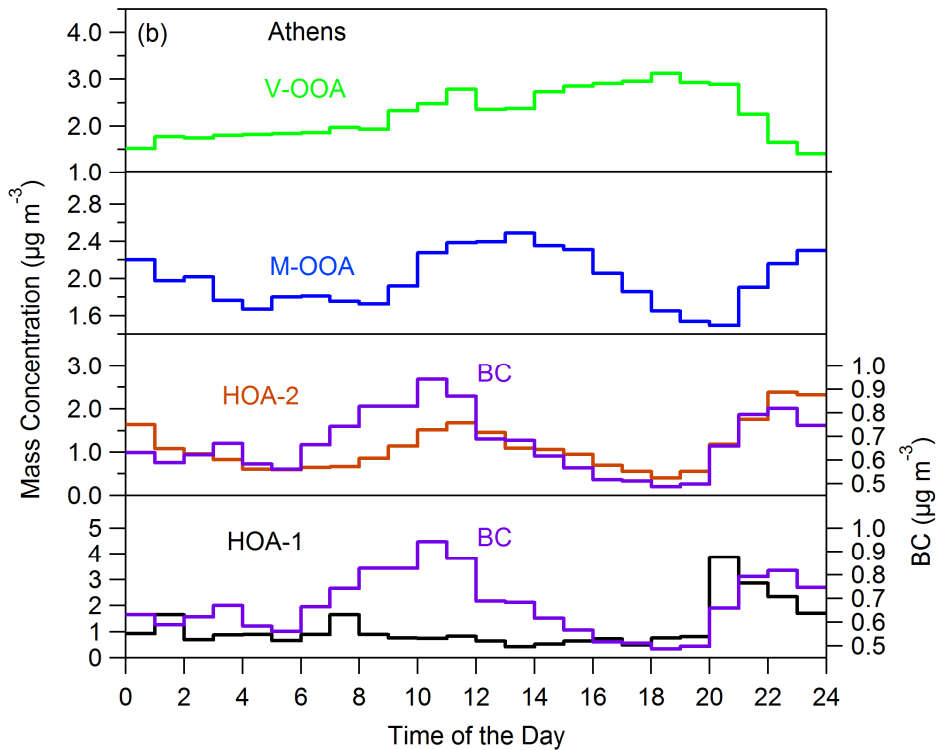
1133

1134

1135

1136
1137 **Figure 4**. Time series a) of the five PMF factors using HR organic mass spectra for
1138 Patras and b) of the four PMF factors found in Athens. For the Patras measurements the
1139 HOA-1 and HOA-2 contribution was very low between the 16th and 23rd of June 2012
1140 due to the high wind speed during that period.

1141

1142
1143
1144 **Figure 5**. Diurnal cycles of the PMF factors a) in Patras and b) in Athens.

1145